The Genome of *Chenopodium ficifolium*: Developing Genetic Resources and a Diploid Model System for Allotetraploid Quinoa

Clayton D. Ludwig[1], Peter J. Maughan[2], Eric N. Jellen[2], Thomas M. Davis[1]

Affiliations:

[1]Department of Agriculture, Nutrition, and Food Systems, University of New Hampshire, Durham, NH 03824, USA

[2]Brigham Young University, Department of Plant and Wildlife Sciences, College of Life Sciences, Provo, UT 84602, USA.

Abbreviations:

AED, annotation edit distance; EST, expressed sequence tag; GO, gene ontology; GWAS, genome wide association study; HCGS, UNH Hubbard Center for Genome Studies; HMW, high molecular weight; MSA, multiple sequence alignment; ONT, Oxford Nanopore Technology; PC, pseudochromosome

Abstract

High-quality nuclear, chloroplast, and preliminary mitochondrial genomes have been assembled and annotated for the B-genome diploid (BB: 2n = 2x = 18) figleaf goosefoot (*Chenopodium ficifolium*). The primary objective was to advance a simplified model system for genetic characterization and improvement of allotetraploid (AABB: 2n = 4x = 36) quinoa (*Chenopodium*

quinoa), a nutritionally valuable, halophytic orphan crop. In addition to its diploidy and favorably small genome size, the *C. ficifolium* model provides a shorter generational period and smaller overall plant size as compared to *C. quinoa*, while displaying relevant agronomic trait variations amenable to gene-trait association studies. The *C. ficifolium* 'Portsmouth' nuclear genome was sequenced using PacBio HiFi Long Read technology and assembled using Hifiasm. After manual adjustments, the final ChenoFicP_1.0 assembly consisted of nine pseudochromosomes spanning 711.5 Mbp, while 22,617 genes were identified and annotated. BUSCO analyses indicated a nuclear genome completeness of 97.5%, and a proteome and transcriptome completeness of 98.4 percent. The chloroplast genome assembly detected two equally represented structural haplotypes differing in the orientation of the Short Single Copy region relative to the Long Single Copy region. Phylogenetic and parentage analyses pointed to an unspecified AA diploid species and away from *C. ficifolium* as the likely maternal chloroplast and mitochondrial genome donor(s) during the initial tetraploidization event in the *C. quinoa* lineage. Using the new ChenoFicP_1.0 reference genome, a GWAS was performed on a previously studied *C. ficifolium* F2 population to further define region(s) implicated in the control of three key agronomic traits: days to flowering, plant height, and branch number. This analysis localized control of all three traits to a 7 Mb interval on pseudochromosome Cf4. This region contains approximately 770 genes, including the *FTL1* locus, thus confirming and extending our prior, single-marker analysis showing association of these three traits with an *FTL1* amplicon length polymorphism. The use of these data to further develop *C. ficifolium* as a model species for genetics and breeding of quinoa serves to expand knowledge and germplasm resources for quinoa improvement.

Introduction

Chenopodium ficifolium (figleaf goosefoot) is a weedy, Old-World B-genome diploid (BB: 2n = 2x = 18) relative of the cultivated allotetraploid (AABB: 2n = 4x = 36) pseudocereal crop quinoa (*Chenopodium quinoa* Willd.) (Walsh *et al.*, 2015; Kolano *et al.*, 2016) and its wild sister AABB tetraploid *Chenopodium berlandieri* (Walsh *et al.*, 2015). The genus *Chenopodium* now resides in the family Amaranthaceae, its former Chenopodiaceae family home having recently been subsumed into the Amaranthaceae (Chase *et al.*, 2016), which also hosts the relevant comparator *Beta vulgaris* (sugar beet). Putatively originating from Eurasia (Walsh *et al.*, 2015), figleaf goosefoot is now widespread in North America, both as a weed of human disturbance and as a naturalized part of disturbed ecosystems. It is one of two recognized potential contributors, or a close relative thereof, of the B subgenome to the *C. quinoa* lineage during its initial tetraploidization event, the other B subgenome candidate being diploid *C. suecicum* (Jellen *et al.*, 2011; Mandák *et al.*, 2012; Walsh *et al.*, 2015; Jarvis *et al.*, 2017). Because figleaf goosefoot potentially contributed the B subgenome to quinoa, or is an extant sister species of the contributor, it is a highly relevant candidate to explore as a diploid model species in relation to quinoa's genetic characterization and breeding, and its study may shed light on specific genes governing domestication-related traits in quinoa (Jellen *et al.*, 2013; Walsh *et al.*, 2015; Kolano *et al.*, 2016; Subedi, Neff and Davis, 2021).

Absent a history of intensive breeding, *C. quinoa* has been categorized as an 'orphan crop' (Lemmon *et al.*, 2018; Kumar and Bhalothia, 2020). However, quinoa is receiving increasing interest from consumers due to its high nutritional value and from agronomists and breeders due to its drought and salt tolerance (Gorinstein *et al.*, 2002; Rojas *et al.*, 2009; Vega-Gálvez *et al.*, 2010; Jacobsen, 2011). These and other attributes make quinoa an attractive candidate for

67 production in regions that cannot sustain the major grain crops. Furthermore, quinoa has the
68 potential to serve as a valuable secondary crop, thereby contributing to food security. Thus, it is
69 an attractive candidate for increased production, justifying investment in development of novel
70 genetics and methods to streamline the breeding process (Jacobsen, 2003; Bazile, Jacobsen and
71 Verniau, 2016).

72 Using *C. ficifolium* as a diploid model species has the potential to accelerate trait dissection and
73 gene identification due to its comparative genetic simplicity; shorter generation time of ~40 days
74 compared to quinoa's 90-120 days (Jacobsen, 1997); profuse flower, pollen, and seed production;
75 and smaller plant size facilitating growth chamber cultivation (Subedi et al., 2021). Building
76 upon prior, foundational studies (Štorchová *et al.*, 2015, 2019), the targeted development of *C.*
77 *ficifolium* as a diploid model species was initiated (Subedi, 2020; Subedi, Neff and Davis, 2021)
78 with a focus on: i) producing intraspecific hybrids and segregating progenies; ii) investigating
79 segregation in domestication-related traits of relevance to *C. quinoa* breeding programs; and iii)
80 detecting gene-trait associations for key genes and traits.

81 In an F_2 segregating population from an initial cross involving *C. ficifolium* accessions from
82 Portsmouth ('P') NH USA, and Quebec City ('QC') Quebec Canada, allelic variation in the
83 *Flowering Locus T-Like 1* (*FTL1*) marker locus was found to be associated with variation in days
84 to flower, plant height, and branch number (Subedi, 2020; Subedi, Neff and Davis, 2021). Using
85 previously designed primers (Cháb *et al.*, 2008; Štorchová *et al.*, 2015) to target and
86 conveniently genotype an indel polymorphism within the *FTL1* gene, it was found that F2 plants
87 homozygous for the 'P' allele flowered on average 12 days earlier than plants homozygous for the
88 'QC' allele, and two days earlier than heterozygotes (Subedi, 2020; Subedi, Neff and Davis,
89 2021). As a likely consequence of their decreased maturation time, 'P' allele homozygotes were

also significantly shorter and had fewer branches than plants of the alternate genotypes. These results strongly implicated the *FTL1* chromosomal region in the control of three agronomically important traits, but did not rule out the possibility of influence from other genomic regions. While genotype-phenotype relationships involving *FTL1* must be further studied at both the diploid and the tetraploid level, this research demonstrates the potential value of *C. ficifolium* as a model system in which to accelerate discovery and characterization of gene-trait relationships. The goal of the work reported here is to expand knowledge and establish foundational genomic resources for the *C. ficifolium* model system.

Materials and Methods

Germplasm

All plant cultivation and phenotyping activities were conducted at the New Hampshire Agricultural Experiment Station (NHAES) at the University of New Hampshire (UNH). Two figleaf goosefoot accessions were employed in this study, both of which have been deposited as seed samples with the USDA North Central Plant Introduction Station (NCRPIS) at Ames Iowa. The 'Portsmouth' ('P') accession (PI 698433) was collected by Erin Neff and Thomas Davis in Portsmouth, New Hampshire, USA (Neff, 2017), while the 'Quebec City' ('QC') accession (PI 698434) was collected by Thomas Davis from Quebec City, Quebec, Canada. Crosses between the 'P' and 'QC' accessions to generate F_1 and F_2 populations, and confirmation of parentage using informative *FTL1* amplicons, were as previously described (Subedi, Neff and Davis, 2021). For purposes of comparison, we also employed in-house-numbered accessions 302-A of AA diploid *C. foggii*, and RB6 of AABB allotetraploid *C. berlandieri* var. *macrocalycium*, which

had been collected by Erin Neff and Thomas Davis in southern Maine (Neff, 2017; Neff, Sullivan and Davis, 2018) and in Rye Beach New Hampshire, respectively; and *C. quinoa* accession QQ065 (PI 614880), obtained from USDA NPGS.

DNA Isolation and Genome Sequencing

Figleaf goosefoot 'P' accession was used to construct the primary *de novo* reference genome assembly. DNA from this accession was isolated at Brigham Young University (BYU) using methods designed to yield high molecular weight (HMW) DNA from plant tissues (Vaillancourt and Buell, 2019). The 'P' accession HMW DNA was sequenced at the BYU DNA Sequencing Center (DNASC) using the PacBio HiFi platform (Eid *et al.*, 2009). In addition, this DNA was used at UNH to generate Nanopore sequence on an Oxford Nanopore Technologies (ONT) R9.4.1 flow cell using a library prepared with a rapid sequencing kit (SQK-RAD004) following methods described by Nanopore entitled “Rapid sequencing gDNA – whole genome amplification”.

Illumina sequence was generated at the UNH Hubbard Center for Genome Studies (HCGS) for the following: for the 'P' and 'QC' accessions of *C. ficifolium*; for 35 F2 generation individuals descended from a 'P' x 'QC' cross that was previously studied and described (Subedi et al., 2021); the RB6 accession of *C. berlandieri* var. *macrocalycium*; and for the 302-A accession of *C. foggii*. DNA for Illumina sequencing was isolated at UNH (Subedi et al., 2021) using a CTAB method described by Torres *et al.* (1993).

Nuclear Genome Assembly

PacBio reads were assembled at BYU using Hifiasm Version v0.18.5-r499 (Cheng *et al.*, 2021, 2022) with default settings. Subsequent assembly and annotation processes were done at UNH, where Inspector (Chen *et al.*, 2021) was used to detect and correct errors in the assembly followed by manual examination and adjustments, yielding the *C. ficifolium* Version 1.0 nuclear reference genome designated as ChenoFicP_1.0. Finally, BUSCO (Manni *et al.*, 2021) and dependencies (Stanke *et al.*, 2008; Camacho *et al.*, 2009; Eddy, 2011; Mirarab, Nguyen and Warnow, 2012; Levy Karin, Mirdita and Söding, 2020; Li, 2023) using default settings and the embryophyta_odb10 database was used to calculate nuclear genome completeness. Telomeres were identified within pseudochromosomes (PCs) with the quarTeT toolkit program TeloExplorer (Lin *et al.*, 2023) and within unplaced contigs using tidk (Brown, la Rosa and Mark, 2023). Centromeric regions were identified using the tool CentroMiner which is supplied with the quarTeT toolkit (Lin *et al.*, 2023). Nuclear genome assembly data was visualized using Circos (Krzywinski *et al.*, 2009) in combination with the deepStats toolkit (Richard, 2019) for track generation.

Nuclear Genome Annotation

Once ChenoFicP_1.0 was finalized, repetitive elements were identified using RepeatModeler (Flynn *et al.*, 2020). Those repetitive elements were then masked using RepeatMasker (Tarailo-graovac and Chen, 2009; Flynn *et al.*, 2020; Storer *et al.*, 2021) as the first step in an annotation pipeline patterned after Card *et al.* (2019). The RepeatMasker scripts calcDivergenceFromAlign.pl and createRepeatLandscape.pl were used to analyze output files,

156 determine repetitive element content, and produce data visualizations. A BRAKER IsoSeq
157 compatible singularity container (Bruuna, Gabriel and Hoff, 2024) was passed the fasta file
158 containing soft-masked repetitive elements and Pacific Biosciences IsoSeq data aligned to the
159 genome using minimap2 (Li, 2018). BRAKER flags were set to use the Viridiplantae OrthoDB
160 database (Kuznetsov *et al.*, 2023) for protein sequence, and the Embryophyta odb10 database
161 (Manni *et al.*, 2021) as the Busco lineage.

162 The resulting GFF3 annotation file was passed to MAKER (Holt and Yandell, 2011) as a
163 prediction GFF file, as were the cds-transcripts and proteins files which were used for EST
164 evidence and protein homology evidence, respectively. MAKER was used to update annotations
165 and to provide Annotation Edit Distance (AED) scores. AED values for the final annotation file
166 were produced using AED_cdf_generator.pl (https://github.com/mscampbell). Once complete,
167 the output files for each pseudochromosome were merged to create one contiguous file. This
168 output file contained gene predictions, however without functional annotations. To integrate
169 functional details and GO terms, BLASTP (Johnson *et al.*, 2008) using the UniProtKB/Swiss-
170 Prot database (Bateman *et al.*, 2015), as well as InterProScan (Jones *et al.*, 2014) were passed the
171 protein file produced by MAKER, and the resulting information was integrated into a single file
172 using the maker_functional_gff and ipr_update_gff commands, and sorted with AGAT (Dainat,
173 Hereñú and Pucholt, 2020), which yielded the final GFF3 annotation file.

174 A genome-wide synteny analysis was performed comparing the ChenoFicP_1.0 assembly to the
175 B subgenome of the *C. quinoa* V2 reference genome (Rey *et al.*, 2023) and to the *Beta vulgaris*
176 EL10.1 reference genome (McGrath *et al.*, 2023). As a co-member of the Amaranthaceae family,
177 diploid (2n = 2x = 18) *B. vulgaris* (sugar beet) has been used in previous genomic comparisons
178 with quinoa (Jarvis *et al.*, 2017; Rey *et al.*, 2023). To produce the synteny analysis, *C. quinoa*

annotations and protein fasta files were downloaded from CoGe (id60716), and *B. vulgaris* files from NCBI (GCF_002917755.1). Annotation files were converted to BED format via agat_convert_sp_gff2bed.pl (Dainat, Hereñú and Pucholt, 2020), before being manually rearranged to comply with requirements for MCScanX_h (Wang *et al.*, 2012). BlastP was used to compare the proteome of *C. ficifolium* with those of *B. vulgaris* and *C. quinoa* (Camacho *et al.*, 2009), yielding two blast output files which were merged and passed to MCScanX_h, along with BED files containing positional information for the genes in the blast files. For this analysis, MCScanX used default filtering parameters. SynVisio (Bandi and Gutwin, 2020) was used to visualize the resulting files, illuminating rearrangements and structural variations.

Chloroplast Genome Assembly and Annotation

The 'P' chloroplast genome was initially assembled from extracted PacBio reads using GetOrganelle v1.7.6.1 (Jin *et al.*, 2020) with dependencies SPAdes (Bankevich *et al.*, 2012), Bowtie2 (Langmead and Salzberg, 2012), BLAST+ (Camacho *et al.*, 2009), and Bandage (Wick *et al.*, 2015), and annotated with the online tool GeSeq (Tillich *et al.*, 2017). GetOrganelle was called using get_organelle_from_reads.py and was supplied with raw PacBio reads using the unpaired '-u' flag. Embplant_pt was selected as the genome type, and the target genome size was set to 150 kb which is the approximate size of the *C. quinoa* chloroplast genome (Hong *et al.*, 2017). For the purpose of determining the relative abundance of each detected haplotype of the 'P' chloroplast genome based on the numbers of supporting Nanopore reads, Cp-hap (Wang, Lanfear and Gaut, 2019) was passed reads produced via an ONT R9.4.1 flow cell as previously noted. The final output file produced from GetOrganelle was passed to GeSeq

201 (https://chlorobox.mpimp-golm.mpg.de/geseq.html) (Tillich *et al.*, 2017) for visualization and
202 annotation.

203

204 **Mitochondrial Genome Assembly and Annotation**

205 A contig from the Hifiasm assembly was identified as mitochondrial by aligning all unplaced
206 contigs to the quinoa mitochondrial reference sequence NC_041093.1 (Maughan *et al.*, 2019)
207 with BWA MEM (Li and Durbin, 2009), and manually selecting a long, well-aligned contig. This
208 contig was used as a seed sequence and passed to a *de novo* organelle assembly pipeline
209 described by Jarvis et al., (2022) to assemble the mitochondrial genome. The pipeline was used
210 in two iterations, initially using the HiFi dataset which produced a contig that was passed to the
211 mitochondrial assembly pipeline in conjunction with the long read Nanopore dataset. The
212 Nanopore dataset was then aligned to this contig using minimap2 (Li, 2018), reads matching GC
213 content and length thresholds were stripped from the alignment file via SeqKit (Shen *et al.*,
214 2016), and these reads were passed to Canu (Koren *et al.*, 2017) for *de novo* assembly. Nanopore
215 reads were later used to resolve assembly structure via comparing alignments to the draft
216 mitogenome assembly. The output contig from Canu was manually circularized by locating
217 regions at the start and end of the file that shared 100 percent sequence identity. The circularized
218 version of the assembly was polished using NextPolish (Hu *et al.*, 2020) and the PacBio read set
219 to correct single nucleotide errors. Annotation was performed by GeSeq. Importantly, GeSeq was
220 set to pass third party mitochondrial NCBI RefSeqs from both *C. quinoa* (NC_041093.1) and
221 *Beta vulgaris* subsp. *vulgaris* (NC_002511.2) to BLAT (Kent, 2002) which used annotations
222 from those genomes to locate and annotate homologs within the *C. ficifolium* mitogenome.

223 **Chloroplast and Mitochondrial Inheritance Patterns in *C. ficifolium***

224 Chloroplast and mitochondrial reference-guided assemblies for 'QC', one F1 individual, and four
225 F2 individuals, were constructed and aligned to the respective 'P' organelle genomes using BWA
226 mem (Li and Durbin, 2009) to identify heritable organelle polymorphisms differentiating the two
227 parents. The resulting SAM files were then converted to BAM, sorted, indexed, and a consensus
228 was called using the respective samtools modules (Danecek *et al.*, 2021). Once BAM files for
229 each individual were converted to fasta, freebayes-parallel (Garrison and Marth, 2012; Tange,
230 2018) was used to call variants. Freebayes-parallel was invoked with options to produce a gVCF
231 file, include genotype qualities, use best n alleles set to 4, and cap read depth to 5000. VCF files
232 were filtered to remove low quality calls using vcffilter from vcflib (Garrison *et al.*, 2022) and
233 bcftools (Danecek *et al.*, 2021). Sites or calls were pruned from the chloroplast multisample vcf
234 file if: a) the average depth across all samples was below 100; b) or the site quality was below
235 998; c) or the genotype quality phred score was below 30; d) or depth for a given sample was
236 below 50; e) or more than half of individuals were not represented; f) or the allele balance was
237 below 25 percent or greater than 75 percent; g) or there was a discrepancy between the number
238 of paired and unpaired reads aligned. The vcf file generated for the mitochondrial genome using
239 the same samples was filtered using the same criteria with the addition of a cap of 3000 on the
240 average depth per sample. The filtering criteria and script were based on those provided by
241 http://www.ddocent.com/filtering/. The resulting filtered vcf files were visualized with IGV
242 (Thorvaldsdóttir, Robinson and Mesirov, 2013).

243

244

245 **Chloroplast and Mitochondrial Genome Ancestries**

246 To illuminate the possible role of *C. ficifolium* in the cpDNA ancestries of allotetraploids *C.*
247 *quinoa* and *C. berlandieri*, a minimal phylogenetic tree was generated using six chloroplast
248 genome (cpDNA) assemblies representing four *Chenopodium* species and including beet (*Beta*
249 *vulgaris*) as an outgroup. The *C. quinoa* and *B. vulgaris* chloroplast genomes used were NCBI
250 accessions MK159176.1 and OU343016.1, respectively. All other accessions included in this
251 analysis were assembled by us *de novo* from raw reads using GetOrganelle (Jin *et al.*, 2020). We
252 assembled the *C. berlandieri* chloroplast genome from Illumina 2x150 PE reads previously
253 uploaded to NCBI by Mark Samuels from the University of Montreal (Accession:
254 PRJNA895488) (Samuels *et al.*, 2023). The *C. ficifolium* 'P' chloroplast genome was *de novo*
255 assembled using sequence data extracted from the PacBio dataset as described above, while the
256 *C. ficifolium* 'QC' and the *C. foggii* 302-A chloroplast genomes were assembled from Illumina
257 data produced at the UNH-HCGS. These assemblies were aligned using Mafft (Katoh and
258 Standley, 2013) with default (auto) settings, and a tree was produced using RAxML V. 8.2.12
259 with the GTRCAT model (Stamatakis, 2014). Trees were visualized with TreeViewer (Bianchini
260 and Sánchez-Baracaldo, 2023).

261 For a parallel purpose, a minimal mitochondrial phylogeny was produced by aligning raw reads,
262 either generated by the HCGS for *C. foggii* 302-A, and 'P' and 'QC' *C. ficifolium* accessions or
263 downloaded from NCBI, to the quinoa mitochondrial reference genome NC_041093.1 (Maughan
264 *et al.*, 2019). *B. vulgaris* (SRR6305245) (McGrath *et al.*, 2023) and *C. berlandieri*
265 (PRJNA895488) (Samuels *et al.*, 2023) read sets were downloaded from NCBI. All read data
266 used in this analysis were trimmed and cleaned with Trimmomatic (Bolger, Lohse and Usadel,
267 2014) using the primer sequence file “TruSeq3-PE-2.fa” invoked with the following settings:

ILLUMINACLIP:TruSeq3-PE-2.fa:2:30:10 LEADING:3 TRAILING:3 SLIDINGWINDOW:4:15 MINLEN:36. FastQC (https://www.bioinformatics.babraham.ac.uk/projects/fastqc/) was used to visualize and validate the Trimmomatic output. These reads were then aligned to the quinoa mitochondrial reference genome (Maughan *et al.*, 2019) using BWA mem (Li and Durbin, 2009). Using Samtools view, sort, index, and consensus (Danecek *et al.*, 2021), the BWA produced SAM file was converted to a fasta file containing the consensus sequence. These six fasta files, those produced from reads plus the quinoa mitogenome file used as a reference in the alignment process, were merged into a multi-fasta and Mafft (Katoh and Standley, 2013) was used with default (auto) settings to produce an MSA. A tree was produced using RAxML V. 8.2.12 (Stamatakis, 2014) with the GTRCAT model and *B. vulgaris* specified as the outgroup.

Genome Wide Association Studies

A subset of 21 'P' x 'QC' F2 individuals chosen from the 35 sequenced at the HCGS on the basis of high read depth were used in a GWAS analysis to locate regions throughout the genome implicated in the control of branch angle, internode length, flowering time, plant height, and number of lateral branches. BWA MEM was used to align reads from F2 individuals to the *C. ficifolium* 'P' V1.0 reference genome. Resulting sam files were converted to bam, sorted, and indexed via samtools (Danecek *et al.*, 2021). GATK AddOrReplaceReadGroups (Van der Auwera and O'Connor, 2020) was called to change read group IDs to reflect the sample name to make variant calling possible. Freebayes-parallel (Garrison and Marth, 2012; Tange, 2018) was used to generate a vcf file containing both InDel and SNP variants for all 35 initial individuals. The resulting vcf file was filtered to remove low quality calls following guidelines from

291 http://www.ddocent.com/filtering/. The filtered vcf data in conjunction with phenotypic data
292 collected by Subedi (2020), and name and positional data extracted from the GFF3 annotation
293 file were supplied to the package vcf2gwas (Vogt, Shirsekar and Weigel, 2022) which produced
294 Manhattan plots and positional data for putatively causative SNPs.

295 A region of interest on Cf4 identified via vcf2gwas was then closely examined with respect to
296 gene content and local synteny and collinearity with the *C. quinoa* V2 assembly (Rey *et al.*,
297 2023). For this purpose, this approximately 7 Mb region of interest was manually excised from
298 the full annotation file associated with our ChenoFicP_1.0 assembly, Revigo (Supek *et al.*, 2011)
299 was used to analyze pathways and relationships of genes with attached GO terms, and gene IDs
300 were used to subset the proteome fasta file. BlastP and MCScanX were used to compare this
301 protein subset to the complete proteome of *C. quinoa* and create a homology file. This file, plus
302 the required concatenated BED files were passed to MCScanX_h, which used default filtering
303 criteria with the exception of MATCH_SIZE, which was set to 9 to only include matches with 10
304 or more collinear genes. The MCScanX pipeline developed by BDX consulting (Wang *et al.*,
305 2024) was used to convert data to a format compatible with Circos (Krzywinski *et al.*, 2009).

306 Results

307 Nuclear Genome Assembly

308 The PacBio HiFi read set from *C. ficifolium* 'P' comprised a total of 26.5 Gb of sequence with an
309 N50 of ~14 Kb. These data were supplied to Hifiasm Version 18, yielding 781 contigs of
310 cumulative length 759,656,873 bp (~760 Mb) with an average read depth of 34.8x (Table 1).

Table 1. Hifiasm assembly statistics.

Statistics of contigs:		Read to Contig alignment:	
Number of contigs	780	Mapping rate /%	100.00
Number of contigs > 10000 bp	780	Split-read rate /%	0.47
Number of contigs >1000000 bp	9	Depth	34.87
Total length	759656810	Mapping rate in large contigs /%	92.05
Total length of contigs >1000000bp	729997343	Split-read rate in large contigs /%	0.46
Longest contig	92986964	Depth in large contigs	33.45
Second longest contig length	85613771	Error and Quality Metrics	
N50	79863811	Small-scale assembly error /per Mbp	0.30
L50	5	QV	62.60

Of these contigs, the largest nine ranged in size from a maximum of 92,986,964 bp down to 70,697,261 bp, while the tenth largest (contig ptg000009l) was 8,313,269 bp (Table 2). The remaining 771 contigs were all much smaller: less than 1 Mbp. On the basis of these size discontinuities, and the prior expectation based on the *C. ficifolium* chromosome number (n = x = 9) (Walsh *et al.*, 2015), the nine largest Hifiasm contigs were defined as comprising the initial pseudochromosome (PC) assembly. These nine PCs were then numbered and oriented to

Table 2. Original contig names, pseudochromosome designations, and contig lengths of the primary assembly plus the two largest unplaced contigs after ptg000009l were appended to Cf7.

Name	Renamed	Initial Length	Final Length
ptg000002l	Cf6	92986964	92986964
ptg000006l	Cf5	85613789	85613789
ptg000005l	Cf3	82834534	82834534
ptg000008l	Cf7	74073315	82386584
ptg000003l	Cf2	79863818	79863818
ptg000001l	Cf8	79853931	79853931
ptg000011l	Cf1	77970451	77970451
ptg000004l	Cf4	77790002	77790002
ptg000007l	Cf9	70697261	70697261
ptg000009l	(Merged with Cf7)	8313269	----------
ptg000020l		871519	871519
ptg000025l		721674	721674

maximize correspondence with the *Beta vulgaris* EL10.1 reference genome (McGrath *et al.*, 2023), as was done previously in the assembly of the quinoa Version 1 assembly (Jarvis *et al.*, 2017). Inspector subsequently identified and corrected three structural errors, and 228 small-scale assembly errors, reporting a QV score of 63.39 after correction for this assembly (Figure 1). The G/C content of this genome is 36.9 percent, and varies between approximately 20 and 80 percent per 100 Kb window (Figure 1 Ring D). G/C rich regions are often centrally located within pseudochromosomes; however centromeric regions on the whole have an average G/C content, with pseudochromosome Cf1 having the highest content with 45.47 percent, and the average across all centromeres being 37.75 percent. When comparing the *C. ficifolium* 'QC' accession to the *C. ficifolium* 'P' assembly (Figure 1 Ring C), the number of SNPs differentiating the two per 100 Kb window ranges from as low as 12 to a maximum of 2,321, or approximately one SNP per 43 bases, as found on PC Cf1 from base 11,800,000 to base 11,900,000.

The initial Hifiasm assembly was telomere-to-telomere for PCs Cf3, Cf4, Cf5, Cf6, Cf8, and Cf9, with Cf1 and Cf2 having only one telomere each, and Cf7 having a partially assembled telomere which was oriented in a backwards direction. A homology search of contig ptg000009l, the only unplaced contig larger than 1 Mbp, relative to the quinoa B subgenome (Rey *et al.*, 2023) revealed that this contig was syntenic to the distal end of quinoa chromosome Cq7B, including a telomeric sequence, and thus directed its placement onto Cf7. Following this adjustment, the final “ChenoFicP_1.0” assembly of nine pseudochromosomes had a total length of 729,997,451 bp (~730 Mb). The CentroMiner package identified one region per chromosome as being centromeric (Supplemental Table 1) and produced positional data. Centromeric and telomeric positional data are provided in Supplemental Table 1. BUSCO completeness of the

343 reference genome without unplaced contigs is 96.7 percent, and with unplaced contigs is 97.2

344 percent (Figure 2B).

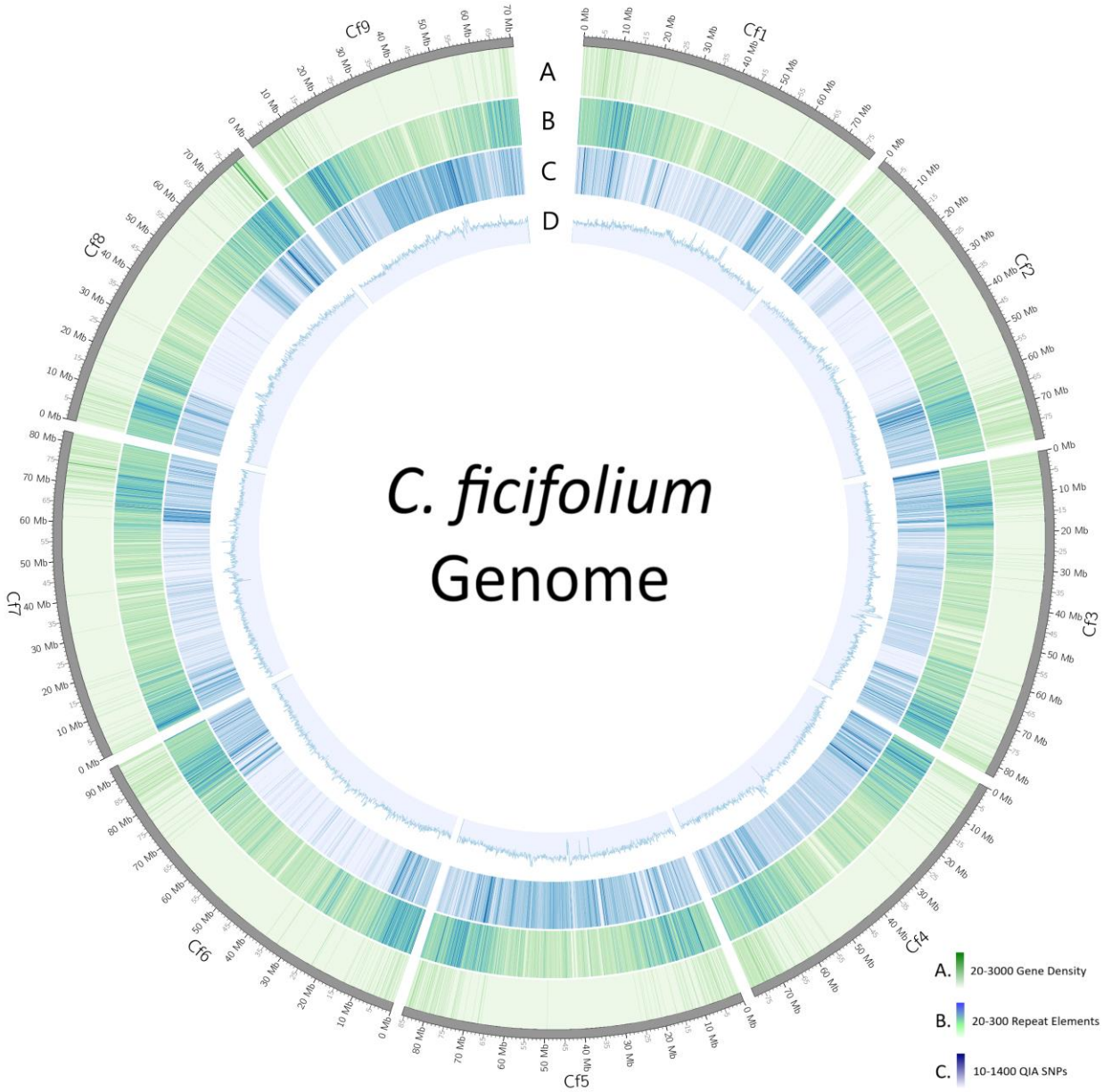

345

346 *Figure 1. This assembly of the C. ficifolium 'UNH_ChenoFicP_1.0' nuclear genome comprises*
347 *nine pseudochromosomes and spans 729.9 Mb.* ***A.*** *Gene density ranging from 20 to 3000 genes*
348 *represented per 100 kb window.* ***B.*** *Repetitive element density ranging from 20 to 300 elements*
349 *per 100 kb window* ***C.*** *SNPs present compared to C. ficifolium accession 'QC' per 100 kb*
350 *window.* ***D.*** *G/C content. Graph represents 20 - 55 percent G/C.*

351 The remaining 771 unplaced contigs comprised a total of about 29.6 Mb, of which 594 contigs
352 (19.6 Mb) and 6 contigs (626 Kb) were subsequently assigned on the basis of sequence
353 homology to the chloroplast and mitochondrial genomes, respectively, leaving a final total of 171
354 contigs (9.4 Mb) unplaced. Further investigation into unplaced contigs using tidk indicated that
355 contigs ptg000020 (871,519 bp) and ptg000025 (721,674 bp) both contain telomeric sequence.
356 These contigs were found by BWA to likely belong on the upstream ends of Cf2 and Cf7
357 respectively; however, they have not been included in the ChenoFicP_1.0 assembly pending
358 further confirmation based upon anticipated long read data.

359

360 **Repetitive Element Identification and Genome Annotation**

361 Data produced by RepeatModeler indicates that 69.9 percent of the ChenoFicP_1.0 genome is
362 comprised of repetitive elements, with the largest contributors being LTR/Gypsy (33.8 percent)
363 and LTR/Copia (11.2 percent) type repetitive sequences, while unknown repeats account for 17.5
364 percent of the total genome fraction. These repetitive elements tend to cluster towards telomeres
365 in (Figure 1 Ring B). Non-repetitive sequence accounts for 30.1 percent of the genome (Figure
366 2A).

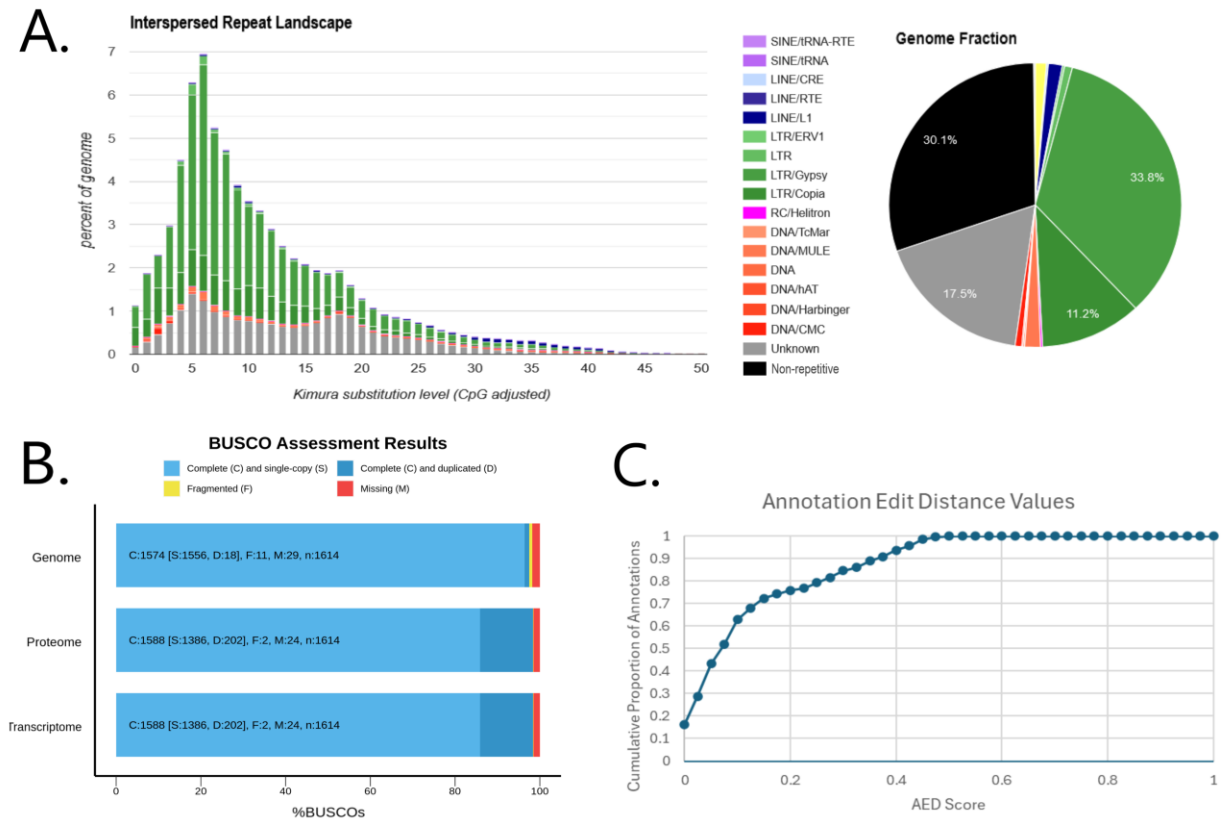

Figure 2 ***A****. Repetitive element analysis and summary graph produced by RepeatModeler. Green: LTR elements, Grey: Unknown repetitive elements, Black: Non-repetitive sequence.* ***B****. BUSCO analyses of completeness for the masked genome used in the annotation process (top), the proteome (middle), and transcriptome (bottom).* ***C****. AED (annotation edit distance) scores of gene reannotations produced by Maker. Lower AED values correspond with higher levels of agreement between the annotation and evidence, with 0 representing perfect agreement between the two.*

The final annotation file was used to calculate relative gene density (Figure 1 Ring A). The BUSCO analysis yielded a transcriptome and proteome completeness of 98.4 percent (Figure 2B). Resultant AED values for the final annotation are graphed in Figure 2C. In total, 22,617 genes were identified and annotated with the average gene length (including introns and UTRs, as defined by Maker utilizing unprocessed mRNA transcripts) being 3,958 bp.

Synteny with Quinoa B-subgenome Chromosomes

The MCScanX synteny analysis of the ChenoFicP_1.0 assembly relative to *B. vulgaris* EL10.1 (McGrath *et al.*, 2023) and the quinoa V2 assembly B-subgenome (Rey *et al.*, 2023) revealed numerous structural variations. In both comparisons, translocational differences tended to involve small distal regions near telomeres. Large inversional differences were revealed in ChenoFicP_1.0 chromosomes Cf1, Cf3, and Cf4 relative to the quinoa B-subgenome homologues, the largest of which was on Cf3 and spanned approximately 63.2 Mb (Figure 3). These inversions were positioned centrally, and in every case for chromosomes Cf1, Cf3, and Cf4 were pericentric.

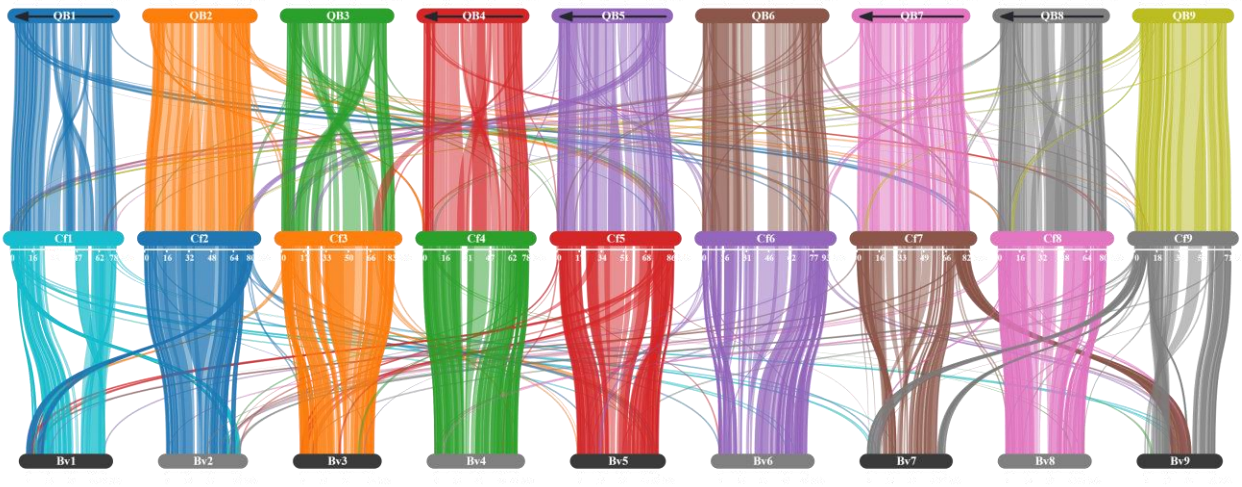

Figure 3. Synteny conservation diagram comparing the assembled pseudochromosomes of C. ficifolium (center) to the B subgenome of quinoa (top), and B. vulgaris EL10.1 (bottom). Chromosomes 1, 4, 5, 7, and 8 of the quinoa B subgenome were manually reoriented (flipped – indicated by arrows) to match those of C. ficifolium for illustrative purposes.

Chloroplast Genome Assembly

GetOrganelle produced two versions of the *C. ficifolium* chloroplast genome assembly, termed "Path 1" and "Path 2", both 151,826 bp in length, but differing in their orientations of the Short Single Copy (SSC) region relative to the Long Single Copy (LSC) region (Figure 4A). When supplied with approximately 263 Mb of Nanopore reads, Cp-hap (Wang, Lanfear and Gaut, 2019) returned approximately equal long read support for both Path 1 (248 reads) and Path 2 (242 reads) orientations, where the Path 2 orientation (Figure 4A, lower) coincided with that of the quinoa chloroplast assembly (MK159176.1) reported by Maughan et al. (2019).

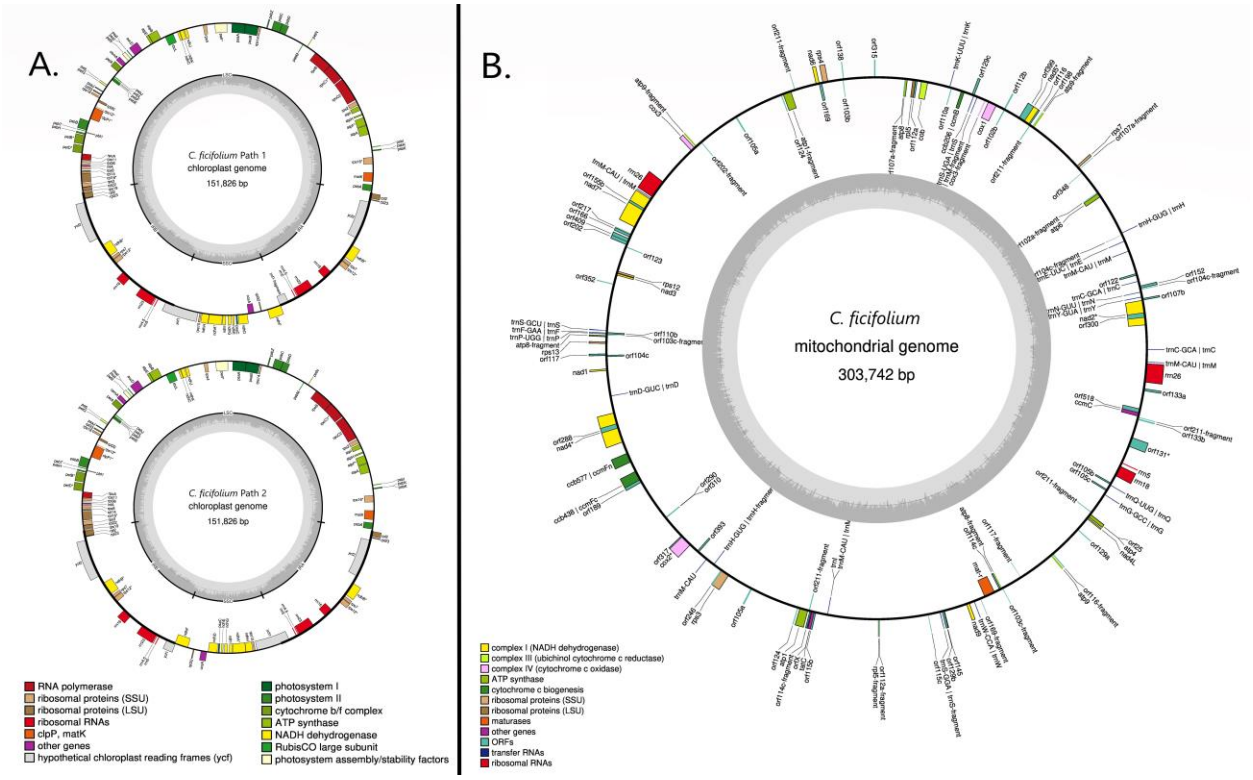

Figure 4 ***A****. Both assembly versions of the C. ficifolium chloroplast genome represented by 'Path 1' and 'Path 2'. These assemblies differ only in the direction of the Short Single Copy region. 'Path 2' (lower) was concordant with the C. quinoa chloroplast genome (MK159176). Genes inside the circle are transcribed in the clockwise direction, genes outside are transcribed counterclockwise.* ***B****. Gene map of the C. ficifolium mitogenome. The mitochondrial genome contains 118 protein coding genes, 23 tRNA genes, and is ~304 Kb in length.*

In both Path 1 and Path 2 orientations, the large single copy region is 83,900 bp, the short single copy is 18,168 bp, and each of the inverted repeat regions are 15,109 bases in length. The chloroplast genome regional boundaries are specified in Table 3. The assembly, including both inverted repeat regions, has a GC content of 37.3 percent and comprises 131 genes, of which there are 86 protein-encoding, 37 tRNA, and 8 rRNA genes. For comparison, the previously published (Kim et al., 2019) *C. ficifolium* chloroplast genome assembly (MK182725) had 129 genes, including 84 protein-encoding, 37 tRNA, and 8 rRNA.

Table 3. Start and end positions of the four regions of the chloroplast assembly. Note that these positions apply to both Path 1 and Path 2 haplotypes; however, the SSC region is inverted in Path 1 relative to Path 2.

Cp Region	Start	End	No. Genes	Protein Encoding
LSC	1	83670	85	63
IR	83671	108779	16	5
SSC	108780	126717	14	13
IR	126718	151826	16	5
		Total	131	86

Mitochondrial Genome Assembly

A 275 kb contig containing a partially assembled mitochondrial genome from the 'P' accession was initially identified from a preliminary Hifiasm assembly. In an iterative sequence seeding process, Nanopore reads were aligned to this contig, extracted from the resulting alignment, assembled *de novo*, and reads were once again aligned. After two rounds of this process, a contig was produced that was manually circularized, and polished with NextPolish using HiFi reads. The resulting 'P' mitochondrial genome assembly has a GC content of 43.8 percent and comprises 90 genes, of which 33 are protein-coding (Figure 4B). The *C. ficifolium* mitochondrial genome assembly is similar in length to that of *C. quinoa* (MK182703), at 303,742 bp versus

433 319,505 bp respectively, and in protein-coding genes, with 33 and 30 respectively (Maughan *et*
434 *al.*, 2019), although these two assemblies display several structural differences.

435

436 **Organelle Genomes' Modes of Transmission**

437 When plastid genome mode of transmission was examined using multisample vcf files
438 containing both parents, 'P' and 'QC', an F1, and four F2 individuals, two distinct sequence
439 haplotypes were revealed. Of the respective polymorphisms, two were single nucleotide indels,
440 while the remaining 17 were SNPs (Supplemental Table 2). The F1 and all F2 individuals share
441 the same sequence haplotype as the maternal parent ('P') as distinct from the 'QC' paternal
442 haplotype (Figure 5A), thereby demonstrating maternal transmission of the chloroplast genome
443 in the 'P' x 'QC' cross used to generate the respective F1 and F2 progenies.

444 To determine the transmission pattern of the mitochondrial genome in the 'P' x 'QC' cross, 'QC'
445 short read alignment to the 'P' mitochondrial reference genome detected nine polymorphisms, of
446 which eight were informative, with the uninformative polymorphism being a SNP for which all
447 individuals had a non-reference nucleotide. Seven of those informative polymorphisms were
448 SNPs, while the eighth was a 22 bp indel (Figure 5B, Supplemental Table 2). These data
449 demonstrate that transmission of the mitochondrial genome in the 'P' x 'QC' cross was maternal.

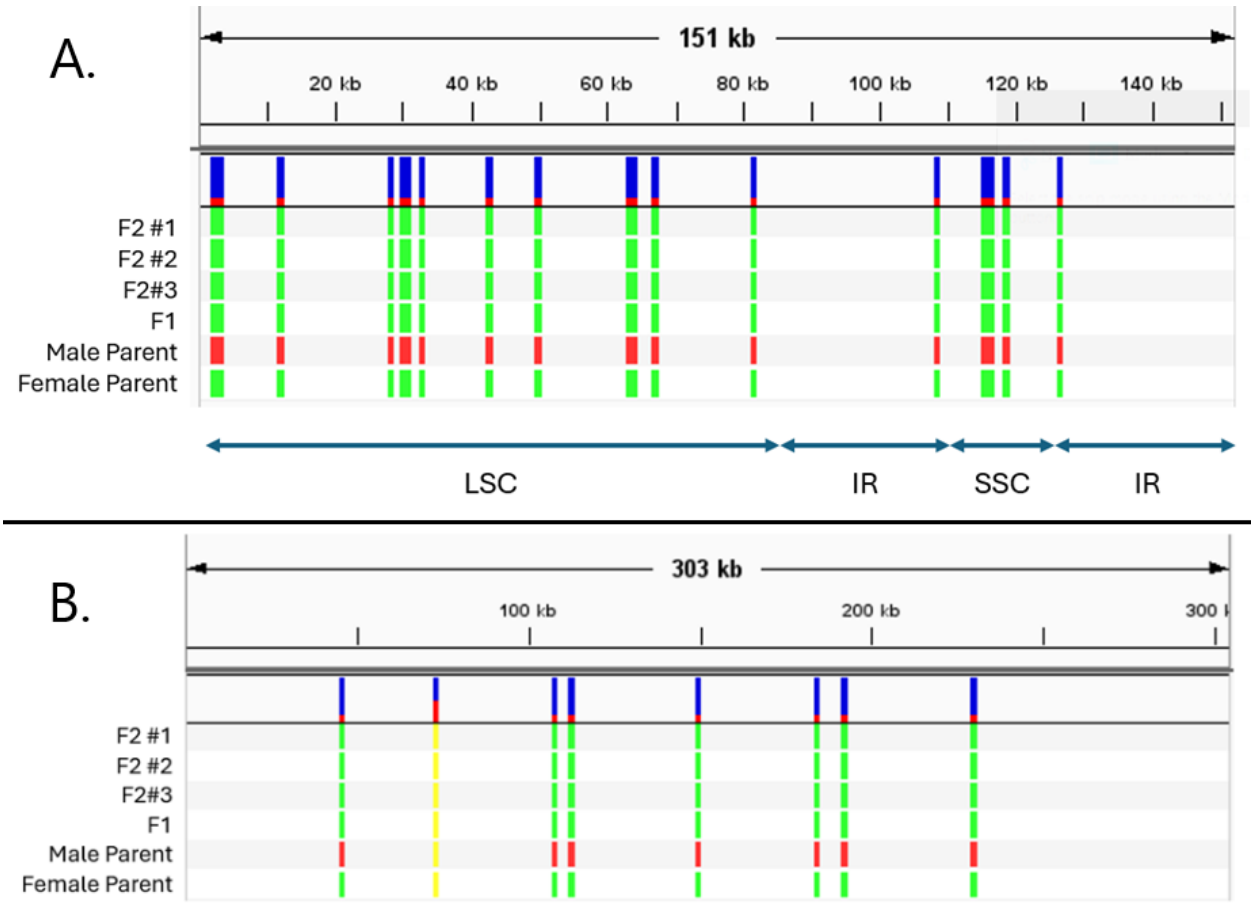

Figure 5 ***A****. Chloroplastic 'Path 2' polymorphisms found among three F2 individuals, one F1 individual, and the maternal ('QC') and paternal ('P') parents in the cross that yielded the F1 individual.* ***B****. Mitochondrial polymorphisms found among three F2 individuals, one F1 individual, and the male and female within the cross that yielded the F1 individual, 'QC' and 'P' respectively. Interestingly one polymorphism shared across all individuals is a heterozygous A/C SNP.*

Chloroplast and Mitochondrial Genome Ancestries

A phylogeny based on *de novo* assembled chloroplast genomes from *B. vulgaris, C. quinoa, C. berlandieri* var. *macrocalycium, C. foggii,* and both the 'P' and 'QC' *C. ficifolium* accessions (Figure 6A) revealed a close affinity of the two *Chenopodium* allotetraploids with the A-genome diploid *C. foggii*, and a more distant relationship with B-genome diploid *C. ficifolium*. Similarly, mitochondrial reference-based assemblies utilizing the same set of germplasm (Figure 6

B) in a narrowly focused phylogeny detected the same pattern of affinities. These outcomes support the prior hypothesis (Maughan *et al.*, 2019) that the organelle genomes of the AABB allotetraploids were both contributed by the AA ancestral diploid.

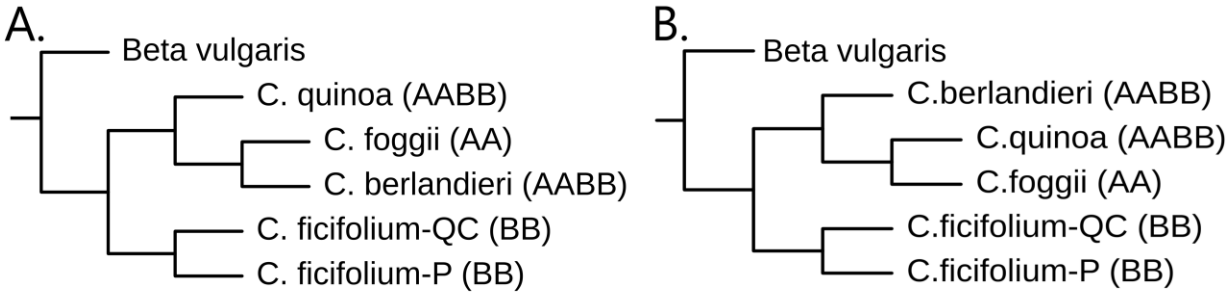

Figure 6 ***A****. Phylogenetic tree illustrating chloroplast genome ancestral relationships among Chenopodium AA and BB diploids and AABB tetraploids in our study. Phylogenetic tree illustrating chloroplast genome ancestral relationships among Chenopodium AA and BB diploids and AABB tetraploids in our study. This phylogenetic tree is based on chloroplast assemblies from C. foggii, both C. ficifolium accessions, C. quinoa, C. berlandieri, and Beta vulgaris which is set as the outgroup.* ***B****. Phylogenetic tree illustrating mitochondrial genome ancestral relationships among Chenopodium AA and BB diploids and AABB tetraploids. This phylogenetic tree was constructed using reference guided assemblies with the C. quinoa mitogenome (NC_041093.1) selected as the reference genome. Beta vulgaris is set as the outgroup.*

Genome Wide Association Study

Of the five trait-specific GWAS analyses performed, two (branch angle and internode length) failed to detect genomic associations. The remaining three traits – days to flowering, plant height, and branch number – were found by GWAS to correlate with a single common region of chromosome Cf4 (Figure 7 A-C). Of these three traits, the correlated SNPs for branch number covered the largest region and fully contained those implicated in the plant height and days to flower analyses. The implicated region spans 7,020,561 bp between positions 70,765,247 and 77,785,808 on Cf4. Features within this region were pulled from the annotation file to create a list of gene names and GO terms associated with those genes. There are 770 annotated genes

487 within the defined region. Of those, 132 were of unknown function. GO terms were assigned to
488 403 genes, including *FTL1*, which at position 74,807,401 – 74,811,571 is number 425 on the list
489 of 770 genes, and is annotated as *Vernalization 3*. *FTL1* had one product classification identified
490 by Interpro (Paysan-Lafosse *et al.*, 2023), being a phosphatidylethanolamine-binding protein
491 (IPR008914).

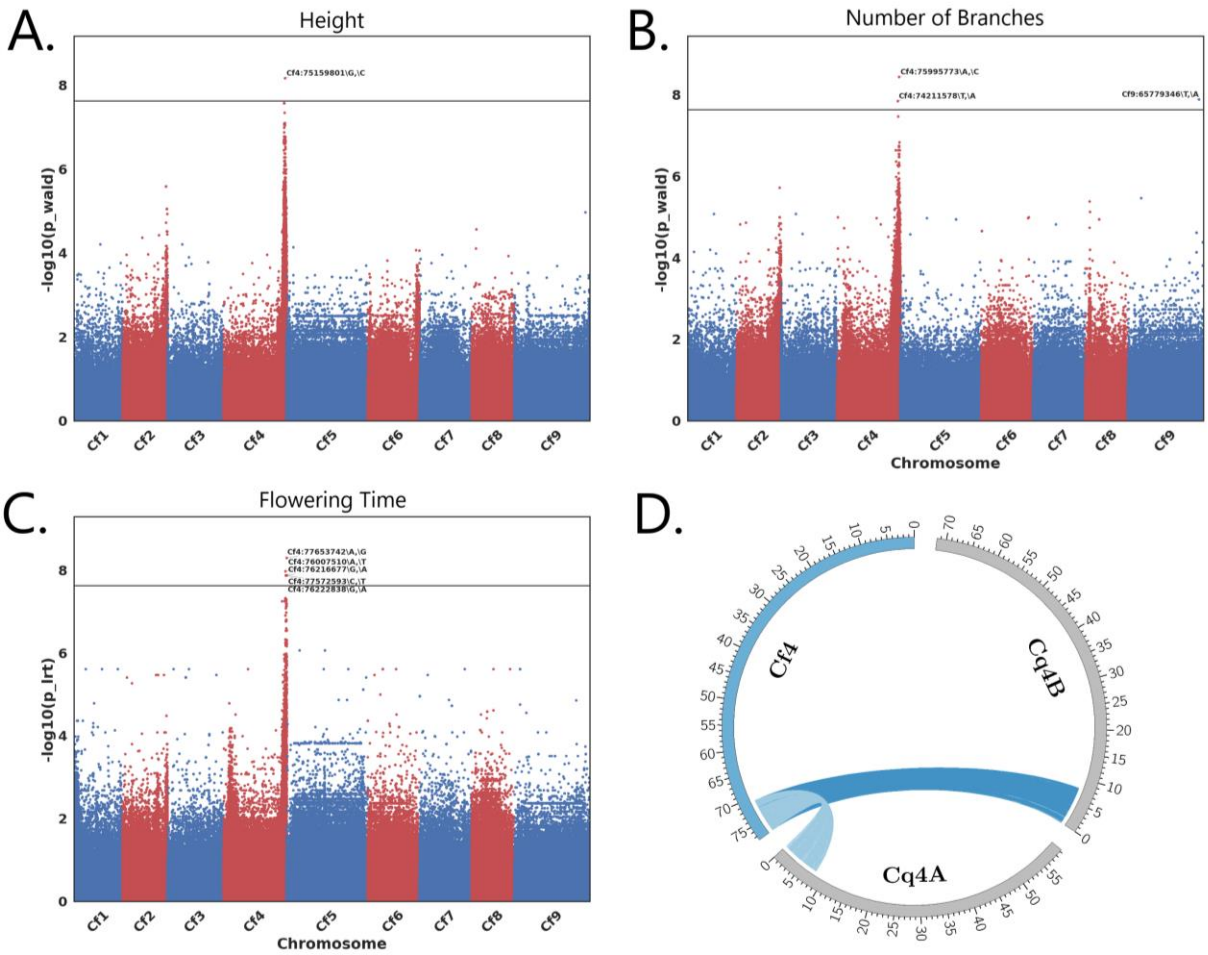

492

493

494 *Figure 7* ***A-C****. GWAS Manhattan plots indicating regions of the genome implicated in the control*
495 *of plant height, number of branches, and flowering time.* ***D****. Synteny analysis of the ~7 Mb region*
496 *found in C. ficifolium Cf4 (Left) implicated by the genome wide association study as compared to*
497 *C. quinoa chromosomes Cq4A and Cq4B as oriented in Rey et al., (2023). Both quinoa*
498 *chromosomes Cq4A and Cq4B are in reverse orientation compared to C. ficifolium chromosome*
499 *Cf4.*

500

501 A microsynteny analysis focusing on the ~7 Mb window implicated in this GWAS was
502 performed to identify homeologs within both *C. quinoa* subgenomes and their locations (Figure 7
503 D). MCScanX identified nine collinear blocks of 10 or more genes from this region in *C.*
504 *ficifolium* that also occur, but in reverse orientation, on quinoa chromosomes Cq4A and Cq4B of
505 the Rey et al., (2023) assembly, as will be discussed later. The analysis of these data indicates
506 that for the 770 genes found in *C. ficifolium* annotation file at this ~7 Mb region, there were 581
507 homoeologous genes found within the *C. quinoa* A subgenome and 610 found within the B
508 subgenome. In total, 107 of the *C. ficifolium* genes within this region are of unknown function
509 and of those, only six have associated GO terms.

510

511 # Discussion

512 **Nuclear Genome**

513 The ChenoFicP_1.0 assembly is the first reference nuclear genome for the *Chenopodium*
514 *ficifolium* diploid model system, and the first diploid *Chenopodium* assembly entirely composed
515 of PacBio HiFi long reads. This reference genome has been developed so that *C. ficifolium* may
516 more effectively serve as a diploid model species for *C. quinoa* genetics and marker-assisted
517 breeding. Pseudochromosomes within this *C. ficifolium* assembly have been numbered to
518 correspond with, and oriented to be syntenic and collinear with, the previously published *Beta*
519 *vulgaris* (2n = 2x = 18) EL10.1 genome (McGrath *et al.*, 2023), thereby following the example
520 of Jarvis et al., (2017) in which the quinoa V1 assembly was similarly oriented. The fact that the
521 quinoa V2 assembly (Rey *et al.*, 2023) did not follow this orientation pattern opens the
522 possibility for some confusion, especially with respect to chromosomes Cq1B, Cq4B, Cq5B,

523 Cq7B and Cq8B, which are presented and numbered in reverse orientation in quinoa V2 as
524 compared with quinoa V1 and beet EL10.1. We have followed the initial orientation approach in
525 anticipation of the forthcoming *Chenopodium* pangenome analysis (Jaggi *et al.*, 2024),which
526 employs the original orientation pattern.

527 Beet was initially selected as the genome comparator for *Chenopodium* because it was the first
528 species to have a published reference genome within the subfamily Chenopodioideae. While the
529 diploid *Spinacia oleracea* (2n = 2x = 12) now has a published genome (Cai *et al.*, 2021), its
530 nuclear genome has only six chromosomes, making comparisons with it suboptimal for
531 identifying syntenic relationships and orienting chromosomes of newly sequenced species.
532 Genome assemblies have been reported for three other *Chenopodium* diploids: the AA diploids
533 *C. pallidicaule* (Jarvis *et al.*, 2017), *C. watsonii* (Young *et al.*, 2023), and the BB diploid *C.*
534 *suecicum* versions 1 (Jarvis et al., 2017) and 2 (Rey et al., 2023). However, to our knowledge, no
535 gene-trait association studies have yet been conducted in these species.

536 The ChenoFicP_1.0 nine-pseudochromosome assembly size of ~730 Mbp incorporates 96% of
537 the 760 Mbp total assembly for the 781 contigs generated by Hifiasm. Cytometrically determined
538 C-values of *C. ficifolium* 'Portsmouth' predict a genome size in the range of 821 to 831 Mbp
539 (Neff, 2017). For comparison, the nine B-subgenome pseudochromosomes of the quinoa
540 assembly sum to 670 Mbp in length (Rey *et al.*, 2023), or approximately 8% smaller than the
541 ChenoFicP_1.0 assembly. Similarly, the nine pseudochromosomes of the quinoa A subgenome
542 sum to 531 Mbp (Rey *et al.*, 2023), which is 3% smaller than the diploid *C. watsonii* 548 Mbp A-
543 genome assembly (Young *et al.*, 2023). An earlier, broad survey of *Chenopodium* germplasm
544 reported C values of 893 Mbp for a Eurasian accession of *C. ficifolium*, 645 Mbp for *C. watsonii*,
545 and 1.545 Gbp for *C. quinoa* (Mandák *et al.*, 2016) Thus, all three of the aforementioned

546 *Chenopodium* genome assemblies are somewhat smaller than the size predicted by cytometric
547 assay. It has been speculated that this pattern of discrepancy may be due to incomplete assembly
548 coverage of some repetitive regions (Young et al., 2023), or it could be due to a consistent
549 technical artifact of flow cytometric analyses.

550 The ChenoFicP_1.0 genome contains 22,617 genes (total genes), of which 5,060 encode proteins
551 that have yet to be characterized within the UniProtKB/Swiss-Prot database. Gene density is
552 greatest in the distal regions of chromosomes (Figure 1 Ring A). For comparison, the total gene
553 counts of the *C. quinoa* A and B subgenomes are 25,913 and 26,942 respectively (Rey *et al.*,
554 2023), the AA diploid *C. watsonii* count was 30,325 (Young *et al.*, 2023), and the BB diploid *C.*
555 *suecicum* count was 29,702 (Rey *et al.*, 2023). Compared with the ChenoFicP_1.0 assembly, the
556 total number of annotated genes within the *C. quinoa* B subgenome is approximately 19.1
557 percent higher. Given that different gene count methodologies were used in these various studies,
558 the observed differences in gene counts among subgenomes and species should be interpreted
559 with caution.

560 RepeatModeler indicated that repetitive elements account for approximately 70 percent (510
561 Mbp) of the *C. ficifolium* genome. For comparison, the quinoa repetitive element content was
562 approximately 65% for the total genome (Zou *et al.*, 2017; Rey *et al.*, 2023), and approximately
563 63% (421 Mbp) for the B subgenome, with the largest contributors being long terminal repeat
564 retrotransposons representing 46 percent of the total genome size. Over half of the *C. ficifolium*
565 repetitive elements are retrotransposons that cluster towards the center of chromosomes (Figure 1
566 Ring B). These data indicate that there has been some change in the repetitive element landscape
567 in *C. ficifolium* and/or the *C. quinoa* B subgenome subsequent to the quinoa allotetraploid
568 speciation event.

569

570 **Organelle Genome Assemblies**

571 The generation of two different chloroplast genome assembly versions, designated Paths 1 and 2,
572 was an unexpected outcome. Prior chloroplast genome assemblies in *Chenopodium*, including *C.*
573 *quinoa* (Maughan *et al.*, 2019; Gao *et al.*, 2021) and *C. ficifolium* (Kim, Chung and Park, 2019),
574 and in the broader Amaranthaceae family (Chaney *et al.*, 2016; Dong *et al.*, 2016; Kim, Chung
575 and Park, 2019; Ding *et al.*, 2021) including sugar beet (McGrath *et al.*, 2023), have reported
576 only a single chloroplast genome configuration, corresponding to our Path 2 assembly, although
577 Kim et al. (2019b) mention the need to reposition the SSC and LSC regions of the quinoa
578 accession 'Real Blanca' for their alignment procedure, indicating a disagreement in SSC and/or
579 LSC orientation when compared to other assemblies. However, recent literature (Wang, Lanfear
580 and Gaut, 2019) (and citations therein) has established that chloroplast genomes do indeed exist
581 in two equally represented alternate configurations in many if not most plant species, as has now
582 become evident in *Chenopodium*, and that the detection of these alternate forms is enhanced by
583 employment of long read sequencing technologies such as PacBio HiFi and Nanopore. The very
584 long and accurate reads now available from Nanopore technology will be of particular value in
585 relation to mitochondrial genomes, the potential alternate forms of which are often challenging to
586 assemble (Kozik *et al.*, 2019). Given the known complexities of mitochondrial genome
587 organization, the assembly configuration that we present here should be viewed as preliminary
588 and subject to revision.

589

590

591 **Organelle Transmission Patterns**

592 In the absence of evidence to the contrary, organelle genomes are generally assumed to be
593 transmitted maternally in Angiosperms: however, exceptions have been reported (Davis *et al.*,
594 2010), including paternal chloroplast transmission in some *Actinidia* hybrids (Testolin and
595 Cipriani, 1997). Until very recently (Maughan *et al.*, 2024), empirical documentation of modes
596 of organelle inheritance in *Chenopodium* appears to have been limited to a single study involving
597 atrazine resistance in *Chenopodium album* (Warwick and Black, 1980; Corriveau and Coleman,
598 1988; Harris and Ingram, 1991; Kolano *et al.*, 2016). Our analysis agrees with this prior study in
599 its finding of maternal transmission of both chloroplast and mitochondrial markers in our diploid
600 level *C. ficifolium* cross. Similarly, Maughan et al. (2024) have documented the maternal
601 transmission of the organelle genomes in several tetraploid level *Chenopodium* crosses.

602

603 **Organelle Genome Ancestries**

604 Although *C. ficifolium* is a candidate B nuclear genome donor in the initial hybridization that
605 formed quinoa 3.3 to 6.3 million years ago (Štorchová *et al.*, 2015; Kolano *et al.*, 2016; Jarvis *et*
606 *al.*, 2017; Maughan *et al.*, 2019), prior analyses indicate that a BB diploid was not the ancestral
607 donor of the allotetraploids' organelle genomes (Maughan *et al.*, 2019). Instead, that role has
608 been assigned to the A nuclear genome donor (Maughan *et al.*, 2019). That assignment is
609 supported by our chloroplast and mitochondrial minimal phylogenies, which both place *C.*
610 *ficifolium* as sister to a clade consisting of AABB tetraploids and an AA diploid.

611 It is considered likely that, in the initial AABB hybridization event, the ancestral AA
612 diploid served as female and maternal organelle genome donor (Maughan *et al.*, 2019).

613 Documentation of such in our *C. ficifolium* cross and in tetraploid level crosses (Maughan *et al.*,
614 2024) strengthens the thesis that the original hybridization event was of the form AA x BB, i.e.,
615 with the AA diploid ancestor serving as female. Final validation of this model will await the
616 analysis of organelle genome transmission in reciprocal crosses between AA and BB diploids.

617

618 **Genome Wide Association Studies**

619 The data produced from these genome-wide analyses indicate that, in the studied segregating
620 population, variation in the agronomically important traits of days to flower, plant height, and
621 branch number were predominantly, if not entirely, under the control of one or more genes within
622 a single, 7 Mb region located towards the bottom of pseudochromosome Cf4 and containing the
623 *FTL1* locus previously employed as a marker by Subedi et al. (2021). Our genome-wide analysis
624 extends the findings of Subedi *et al*. (2021) by focusing attention on this Cf4 "hot spot" and the
625 genes residing therein. Of note, the association of branch angle with a single SNP on Cf9 was not
626 further investigated due to its presumed spurious nature. Manhattan plots will typically associate
627 a number of SNPs within and surrounding a causative region, and this questionable SNP did not
628 have any significantly associated markers adjacent to it, nor was it seen in the other two analyses
629 investigating plant height or days to flower.

630 Gene ontology data submitted to Revigo indicated the presence of a myriad of genes responsible
631 for controlling functions that are not intrinsically associated with these traits of interest; however,
632 this region contains *Flowering Locus T-Like 1* (*FTL1*), which was automatically annotated as
633 *Vernalization 3* (*VRN3*) within the GFF file. This gene is between positions 74,807,401 and
634 74,811,571, placing it centrally within the denoted significance region on Cf4. *FTL1* had one

635 product classification identified by Interpro (Paysan-Lafosse *et al.*, 2023), being a
636 phosphatidylethanolamine-binding protein (IPR008914).

637 To further understand relationships between *C. ficifolium* and *C. quinoa,* and functionally utilize
638 *C. ficifolium* as a model species, BlastP and MCScanX microsynteny analyses were performed to
639 investigate relative gene locations across species and subgenomes (Figure 7D). When comparing
640 the *C. ficifolium* region of interest to both of the quinoa subgenomes, all homologous genes in
641 syntenic blocks of ten or more genes were found to reside in corresponding distal regions of
642 quinoa chromosomes Cq4A and Cq4B, reflecting substantial gene order and location
643 conservation within the respective genomic window. This analysis identified quinoa genes
644 CQ035263 (A subgenome) and CQ019992 (B subgenome) within the *C. quinoa* V2 annotation
645 (GFF3) file as being homologous to *C. ficifolium VRN3* (*FTL1*). The product of CQ035263 was
646 queried with BlastP and has an 83 percent sequence identity match to XP_021772286.1, *C.*
647 *quinoa FLOWERING LOCUS T-like*. Similarly, the product of gene CQ019992 is identical to
648 XP_021734330.1. *C. quinoa FLOWERING LOCUS T-like* has a 97% protein identity with the
649 annotated *C. ficifolium* gene Cfic_20093. The data produced using *C. ficifolium* as a model
650 organism for *C. quinoa* via this pipeline has been demonstrated to be an efficacious way of
651 establishing gene-trait relationships via GWAS and locating syntenic regions across species that
652 may be worth investigating to understand agronomically relevant traits. Further investigation of
653 genes within this region is required, perhaps in conjunction with more high-depth sequence data
654 and additional plants to facilitate a fine-mapping study; however, these data are strongly
655 indicative of one or more genes within this region as being implicated in the control of these
656 traits. Further research, likely employing gene editing or transformation methods, is required to
657 test this hypothesis and firmly establish this relationship.

658 The results of this study, in particular the synteny and collinearity analysis comparing *C.*
659 *ficifolium* and quinoa 'QQ74' chromosomes, presents intriguing hints regarding the potential
660 usefulness of figleaf goosefoot as a breeding resource for quinoa improvement. The primary
661 structural variants differentiating the B genome chromosomes in these two species are three large
662 pericentric inversions. However, the largest of these, on chromosome Cq3B, was a
663 rearrangement present only in a subset of quinoa lines derived from lowland Chilean germplasm,
664 with at least 80% of quinoa lines expected to have collinear Cq3B in comparison with figleaf
665 goosefoot (Rey *et al.* 2023). The remaining two inversions, on Cq1B and Cq4B, appear to have
666 breakpoints extending less than halfway out into their respective chromosome arms, such that
667 they do not encompass recombinogenic regions (Maughan *et al.* 2024). Consequently, while
668 triploid (AB_qB_f) figleaf goosefoot x quinoa hybrids are expected to be highly sterile, backcross
669 hybrids might theoretically be recoverable and, if so, we might expect a high degree of pairing
670 and recombination between their B genomes. This approach – crossing of the polyploid crop to
671 its wild, diploid progenitor - has been successfully employed to introduce numerous resistance
672 genes from the wild progenitor goatgrass (*Aegilops tauschii*, DD) into bread wheat (*Triticum*
673 *aestivum*, AABBDD) while restricting recombination, and consequently undesirable linkage
674 drag, to a single subgenome (Cox, Raupp and Gill, 1994).

675 **Conclusion**

676 The development of high-quality annotated reference nuclear and chloroplast genomes
677 and a preliminary mitochondrial genome for *C. ficifolium* serves as a foundational advance in the
678 development of this species as a BB diploid model system for related allotetraploids of interest,
679 with a primary focus on *C. quinoa* and *C. berlandieri.* Looking ahead, next steps in the
680 development and implementation of this model system include: broadening the germplasm base

via plant collection in diverse environments; establishing new hybrids and populations segregating for additional traits of interest including male sterility (Ward, 1998), and disease resistance, specifically downy mildew (Nolen *et al.*, 2022); and the establishment of effective protocols for gene editing and *in vitro* culture and regeneration for both quinoa and its diploid model(s), with immediate focus on manipulation of *FTL1*. The fact that the organelle genomes present in allotetraploid quinoa were likely derived via maternal transmission from its AA diploid ancestor, not from its BB ancestor, points to the need for parallel development of an AA diploid model system in *Chenopodium*. Foundational steps in this direction have already been taken via the generation of genome assemblies for AA diploids *C. pallidicaule* (Mangelson *et al.*, 2019) and *C. watsonii* (Young *et al.*, 2023), and useful germplasm collection in *C. foggii* (Neff, Sullivan and Davis, 2018). As yet, to our knowledge, no genetic crosses or segregating progeny populations have yet been generated in an AA diploid, so this should be a top priority going forward. Finally, opportunity exists for breeding of quinoa with figleaf goosefoot, either by backcrossing of AB_qB_f triploid hybrids as females or through the generation of synthetic allotetraploids by chromosome doubling of these triploid hybrids.

Acknowledgements

The research reported in this publication was partially funded by the New Hampshire Agricultural Experiment Station. This is Scientific Contribution Number 3032. This work is/was supported by the USDA National Institute of Food and Agriculture (Hatch) Project NH00678 (accession number 1019990), and by USDA NIFA project 110390. Ed Wilcox and the BYU DNASC (RRID: SCR_017781) provided sequencing support".

Conflicts of Interest

These authors have not declared any conflicts of interest.

ORCID iDs

Clayton D. Ludwig https://orcid.org/0009-0004-8921-2479

Peter J. Maughan https://orcid.org/0000-0003-3714-3411

Eric N. Jellen https://orcid.org/0000-0002-7906-4845

Thomas M. Davis https://orcid.org/0000-0001-5455-0524

Data Availability

Genome and sequence datasets are available from NCBI using IDs SUB12919328 and SRR28959327, respectively. This genome can be found using the search term "UNH_ChenoFicP_1.0". This assembly, annotation data in GFF3 format, and supplemental annotation files can be accessed via figshare.com: https://doi.org/10.6084/m9.figshare.c.7590620

References

Van der Auwera, G.A. and O'Connor, B.D. (2020) *Genomics in the cloud: using Docker, GATK, and WDL in Terra*. O'Reilly Media.

Bandi, V. and Gutwin, C. (2020) 'Interactive exploration of genomic conservation', *Proceedings - Graphics Interface*, 2020-May.

Bankevich, A. *et al.* (2012) 'SPAdes: A new genome assembly algorithm and its applications to single-cell sequencing', *Journal of Computational Biology*, 19(5), pp. 455–477. Available at: https://doi.org/10.1089/cmb.2012.0021.

Bateman, A. *et al.* (2015) 'UniProt: A hub for protein information', *Nucleic Acids Research*, 43(D1), pp. D204–D212. Available at: https://doi.org/10.1093/nar/gku989.

Bazile, D., Jacobsen, S.-E. and Verniau, A. (2016) 'The Global Expansion of Quinoa: Trends and Limits', *Frontiers in Plant Science*, 7(May), pp. 1–6. Available at: https://doi.org/10.3389/fpls.2016.00622.

Bianchini, G. and Sánchez-Baracaldo, P. (2023) 'TreeViewer Version 2.1.0'. Zenodo. Available at: https://doi.org/10.5281/zenodo.7768344.

Bolger, A.M., Lohse, M. and Usadel, B. (2014) 'Trimmomatic: A flexible trimmer for Illumina sequence data', *Bioinformatics*, 30(15), pp. 2114–2120. Available at: https://doi.org/10.1093/bioinformatics/btu170.

Brown, M., la Rosa, P.M. and Mark, B. (2023) 'A Telomere Identification Toolkit'. Zenodo. Available at: https://doi.org/10.5281/zenodo.10091385.

Bruuna, T., Gabriel, L. and Hoff, K.J. (2024) 'Navigating Eukaryotic Genome Annotation Pipelines: A Route Map to BRAKER, Galba, and TSEBRA', *arXiv preprint arXiv:2403.19416* [Preprint].

Cai, X. *et al.* (2021) 'Genomic analyses provide insights into spinach domestication and the genetic basis of agronomic traits', *Nature Communications*, 12(1), p. 7246. Available at: https://doi.org/10.1038/s41467-021-27432-z.

Camacho, C. *et al.* (2009) 'BLAST+: Architecture and applications', *BMC Bioinformatics*, 10, pp. 1–9. Available at: https://doi.org/10.1186/1471-2105-10-421.

Card, D.C. *et al.* (2019) 'GBE Genomic Basis of Convergent Island Phenotypes in Boa Constrictors', 11(11), pp. 3123–3143. Available at: https://doi.org/10.1093/gbe/evz226.

Cháb, D. *et al.* (2008) 'Two FLOWERING LOCUS T (FT) homologs in Chenopodium rubrum differ in expression patterns', *Planta*, 228(6), pp. 929–940. Available at: https://doi.org/10.1007/s00425-008-0792-3.

Chaney, L. *et al.* (2016) ' The complete chloroplast genome sequences for four Amaranthus species (Amaranthaceae) ', *Applications in Plant Sciences*, 4(9), pp. 4–9. Available at: https://doi.org/10.3732/apps.1600063.

Chase, M.W. *et al.* (2016) 'An update of the Angiosperm Phylogeny Group classification for the

orders and families of flowering plants: APG IV', *Botanical Journal of the Linnean Society*, 181(1), pp. 1–20. Available at: https://doi.org/10.1111/boj.12385.

Chen, Y. *et al.* (2021) 'Accurate long-read de novo assembly evaluation with Inspector', *Genome Biology*, 22(1), pp. 1–21. Available at: https://doi.org/10.1186/s13059-021-02527-4.

Cheng, H. *et al.* (2021) 'Haplotype-resolved de novo assembly using phased assembly graphs with hifiasm', *Nature Methods*, 18(2), pp. 170–175. Available at: https://doi.org/10.1038/s41592-020-01056-5.

Cheng, H. *et al.* (2022) 'Haplotype-resolved assembly of diploid genomes without parental data', *Nature Biotechnology*, 40(9), pp. 1332–1335. Available at: https://doi.org/10.1038/s41587-022-01261-x.

Corriveau, J.L. and Coleman, A.W. (1988) 'Rapid screening method to detect potential biparental inheritance of plastid DNA and results for over 200 angiosperm species', *American Journal of Botany*, 75(10), pp. 1443–1458. Available at: https://doi.org/https://doi.org/10.1002/j.1537-2197.1988.tb11219.x.

Cox, T.S., Raupp, W.J. and Gill, B.S. (1994) 'Leaf rust-resistance genes Lr41, Lr42, and Lr43 transferred from Triticum tauschii to common wheat', *Crop science*, 34(2), pp. 339–343.

Dainat, J., Hereñú, D. and Pucholt, P. (2020) 'AGAT: Another Gff Analysis Toolkit to handle annotations in any GTF', *GFF format. Zenodo*, 431.

Danecek, P. *et al.* (2021) 'Twelve years of SAMtools and BCFtools', *GigaScience*, 10(2), pp. 1–4. Available at: https://doi.org/10.1093/gigascience/giab008.

Davis, T.M. *et al.* (2010) 'Chloroplast DNA inheritance, ancestry, and sequencing in Fragaria', *Acta Hort*, 859, pp. 221–228. Available at: http://www.actahort.org/books/859/859_25.htm.

Ding, D. Bin *et al.* (2021) 'Characterization and phylogenetic analysis of the complete chloroplast genome of Amaranthus viridis (Amaranthaceae)', *Mitochondrial DNA Part B: Resources*, 6(9), pp. 2610–2612. Available at: https://doi.org/10.1080/23802359.2021.1961631.

Dong, W. *et al.* (2016) 'Comparative analysis of the complete chloroplast genome sequences in psammophytic Haloxylon species (Amaranthaceae)', *PeerJ*, 2016(11), pp. 1–21. Available at: https://doi.org/10.7717/peerj.2699.

Eddy, S.R. (2011) 'Accelerated profile HMM searches', *PLoS Computational Biology*, 7(10). Available at: https://doi.org/10.1371/journal.pcbi.1002195.

Eid, J. *et al.* (2009) 'Real-time DNA sequencing from single polymerase molecules', *Science*, 323(5910), pp. 133–138. Available at: https://doi.org/10.1126/science.1162986.

Flynn, J.M. *et al.* (2020) 'RepeatModeler2 for automated genomic discovery of transposable element families', *Proceedings of the National Academy of Sciences of the United States of America*, 117(17), pp. 9451–9457. Available at: https://doi.org/10.1073/pnas.1921046117.

Gao, M.Z. *et al.* (2021) 'Complete chloroplast genome of the grain Chenopodium quinoa Willd., an important economical and dietary plant', *Mitochondrial DNA Part B: Resources*, 6(1), pp. 40–42. Available at: https://doi.org/10.1080/23802359.2020.1845107.

800 Garrison, E. *et al.* (2022) 'A spectrum of free software tools for processing the VCF variant call
801 format: vcflib, bio-vcf, cyvcf2, hts-nim and slivar', *PLoS Computational Biology*, 18(5), pp. 1–
802 14. Available at: https://doi.org/10.1371/journal.pcbi.1009123.

803 Garrison, E. and Marth, G. (2012) 'Haplotype-based variant detection from short-read
804 sequencing', pp. 1–9. Available at: http://arxiv.org/abs/1207.3907.

805 Gorinstein, S. *et al.* (2002) 'Characterisation of pseudocereal and cereal proteins by protein and
806 amino acid analyses', *Journal of the Science of Food and Agriculture*, 82(8), pp. 886–891.
807 Available at: https://doi.org/10.1002/jsfa.1120.

808 Harris, S.A. and Ingram, R. (1991) 'Chloroplast DNA and biosystematics: The effects of
809 intraspecific diversity and plastid transmission', *TAXON*, 40(3), pp. 393–412. Available at:
810 https://doi.org/https://doi.org/10.2307/1223218.

811 Holt, C. and Yandell, M. (2011) 'MAKER2: An annotation pipeline and genome-database
812 management tool for second-generation genome projects', *BMC Bioinformatics*, 12(1), p. 491.
813 Available at: https://doi.org/10.1186/1471-2105-12-491.

814 Hong, S.Y. *et al.* (2017) 'Complete chloroplast genome sequences and comparative analysis of
815 Chenopodium quinoa and C. Album', *Frontiers in Plant Science*, 8(October), pp. 1–12.
816 Available at: https://doi.org/10.3389/fpls.2017.01696.

817 Hu, J. *et al.* (2020) 'NextPolish: A fast and efficient genome polishing tool for long-read
818 assembly', *Bioinformatics*, 36(7), pp. 2253–2255. Available at:
819 https://doi.org/10.1093/bioinformatics/btz891.

820 Jacobsen, S.E. (1997) 'Adaptation of quinoa (Chenopodium quinoa) to Northern European
821 agriculture: Studies on developmental pattern', *Euphytica*, 96(1), pp. 41–48. Available at:
822 https://doi.org/10.1023/A:1002992718009.

823 Jacobsen, S.E. (2003) 'The worldwide potential for quinoa (Chenopodium quinoa Willd.)', *Food*
824 *Reviews International*, 19(1–2), pp. 167–177. Available at: https://doi.org/10.1081/FRI-
825 120018883.

826 Jacobsen, S.E. (2011) 'The Situation for Quinoa and Its Production in Southern Bolivia: From
827 Economic Success to Environmental Disaster', *Journal of Agronomy and Crop Science*, 197(5),
828 pp. 390–399. Available at: https://doi.org/10.1111/j.1439-037X.2011.00475.x.

829 Jaggi, K.E. *et al.* (2024) 'A Pangenome Reveals LTR Repeat Dynamics as a Major Driver of
830 Genome Evolution in Chenopodium', *The Plant Genome* [Preprint].

831 Jarvis, D.E. *et al.* (2017) 'The genome of Chenopodium quinoa', *Nature*, 542(7641), pp. 307–
832 312. Available at: https://doi.org/10.1038/nature21370.

833 Jarvis, D.E. *et al.* (2022) 'Chromosome-Scale Genome Assembly of the Hexaploid Taiwanese
834 Goosefoot "Djulis" (Chenopodium formosanum)', *Genome Biology and Evolution*, 14(8), pp. 1–
835 7. Available at: https://doi.org/10.1093/gbe/evac120.

836 Jellen, E.N. *et al.* (2011) 'Chenopodium', in *Wild Crop Relatives: Genomic and Breeding*
837 *Resources*. Berlin, Heidelberg, Heidelberg: Springer Berlin Heidelberg, pp. 35–61. Available at:
838 https://doi.org/10.1007/978-3-642-14387-8_3.

Jellen, E.N. *et al.* (2013) 'Botany , Phylogeny and Evolution', in *State of the Art Report on Quinoa around the World*. Rome: FAO & CIRAD, pp. 12–23.

Jin, J.J. *et al.* (2020) 'GetOrganelle: A fast and versatile toolkit for accurate de novo assembly of organelle genomes', *Genome Biology*, 21(1), pp. 1–31. Available at: https://doi.org/10.1186/s13059-020-02154-5.

Johnson, M. *et al.* (2008) 'NCBI BLAST: a better web interface.', *Nucleic acids research*, 36(Web Server issue), pp. 5–9. Available at: https://doi.org/10.1093/nar/gkn201.

Jones, P. *et al.* (2014) 'InterProScan 5: Genome-scale protein function classification', *Bioinformatics*, 30(9), pp. 1236–1240. Available at: https://doi.org/10.1093/bioinformatics/btu031.

Katoh, K. and Standley, D.M. (2013) 'MAFFT multiple sequence alignment software version 7: Improvements in performance and usability', *Molecular Biology and Evolution*, 30(4), pp. 772–780. Available at: https://doi.org/10.1093/molbev/mst010.

Kent, W.J. (2002) ' BLAT —The BLAST -Like Alignment Tool ', *Genome Research*, 12(4), pp. 656–664. Available at: https://doi.org/10.1101/gr.229202.

Kim, Y., Chung, Y. and Park, J. (2019) 'The complete chloroplast genome of Chenopodium ficifolium Sm. (Amaranthaceae)', *Mitochondrial DNA Part B: Resources*, 4(1), pp. 872–873. Available at: https://doi.org/10.1080/23802359.2019.1573122.

Kim, Y., Park, J. and Chung, Y. (2019) 'The complete chloroplast genome of Suaeda japonica Makino (Amaranthaceae)', *Mitochondrial DNA Part B: Resources*, 4(1), pp. 1505–1507. Available at: https://doi.org/10.1080/23802359.2019.1601039.

Kolano, B. *et al.* (2016) 'Molecular and cytogenetic evidence for an allotetraploid origin of Chenopodium quinoa and C. berlandieri (Amaranthaceae)', *Molecular Phylogenetics and Evolution*, 100, pp. 109–123. Available at: https://doi.org/10.1016/j.ympev.2016.04.009.

Koren, S. *et al.* (2017) 'Canu: Scalable and accurate long-read assembly via adaptive κ-mer weighting and repeat separation', *Genome Research*, 27(5), pp. 722–736. Available at: https://doi.org/10.1101/gr.215087.116.

Kozik, A. *et al.* (2019) 'The alternative reality of plant mitochondrial DNA: One ring does not rule them all', *PLoS Genetics*, 15(8), pp. 1–30. Available at: https://doi.org/10.1371/journal.pgen.1008373.

Krzywinski, M.I. *et al.* (2009) 'Circos: An information aesthetic for comparative genomics', *Genome Research* [Preprint]. Available at: https://doi.org/10.1101/gr.092759.109.

Kumar, B. and Bhalothia, P. (2020) 'Orphan crops for future food security', *Journal of Biosciences*, 45(1). Available at: https://doi.org/10.1007/s12038-020-00107-5.

Kuznetsov, D. *et al.* (2023) 'OrthoDB v11: annotation of orthologs in the widest sampling of organismal diversity', *Nucleic Acids Research*, 51(1 D), pp. D445–D451. Available at: https://doi.org/10.1093/nar/gkac998.

Langmead, B. and Salzberg, S.L. (2012) 'Fast gapped-read alignment with Bowtie 2', *Nature*

Methods, 9(4), pp. 357–359. Available at: https://doi.org/10.1038/nmeth.1923.

Lemmon, Z.H. *et al.* (2018) 'Rapid improvement of domestication traits in an orphan crop by genome editing', *Nature Plants*, 4(10), pp. 766–770. Available at: https://doi.org/10.1038/s41477-018-0259-x.

Levy Karin, E., Mirdita, M. and Söding, J. (2020) 'MetaEuk-sensitive, high-throughput gene discovery, and annotation for large-scale eukaryotic metagenomics', *Microbiome*, 8(1), pp. 1–15. Available at: https://doi.org/10.1186/s40168-020-00808-x.

Li, H. (2018) 'Minimap2: Pairwise alignment for nucleotide sequences', *Bioinformatics*, 34(18), pp. 3094–3100. Available at: https://doi.org/10.1093/bioinformatics/bty191.

Li, H. (2023) 'Genome analysis Protein-to-genome alignment with miniprot', 39(January), pp. 1–6.

Li, H. and Durbin, R. (2009) 'Fast and accurate short read alignment with Burrows-Wheeler transform', *Bioinformatics*, 25(14), pp. 1754–1760. Available at: https://doi.org/10.1093/bioinformatics/btp324.

Lin, Y. *et al.* (2023) 'QuarTeT: A telomere-To-Telomere toolkit for gap-free genome assembly and centromeric repeat identification', *Horticulture Research*, 10(8), pp. 1–7. Available at: https://doi.org/10.1093/hr/uhad127.

Mandák, B. *et al.* (2012) 'Is hybridization involved in the evolution of the Chenopodium album aggregate? An analysis based on chromosome counts and genome size estimation', *Flora: Morphology, Distribution, Functional Ecology of Plants*, 207(7), pp. 530–540. Available at: https://doi.org/10.1016/j.flora.2012.03.010.

Mandák, B. *et al.* (2016) 'How genome size variation is linked with evolution within Chenopodium sensu lato', *Perspectives in Plant Ecology, Evolution and Systematics*, 23, pp. 18–32. Available at: https://doi.org/10.1016/j.ppees.2016.09.004.

Mangelson, H. *et al.* (2019) 'The genome of Chenopodium pallidicaule: An emerging Andean super grain', *Applications in Plant Sciences*, 7(11), pp. 1–12. Available at: https://doi.org/10.1002/aps3.11300.

Manni, M. *et al.* (2021) 'BUSCO Update: Novel and Streamlined Workflows along with Broader and Deeper Phylogenetic Coverage for Scoring of Eukaryotic, Prokaryotic, and Viral Genomes', *Molecular Biology and Evolution*, 38(10), pp. 4647–4654. Available at: https://doi.org/10.1093/molbev/msab199.

Maughan, P.J. *et al.* (2019) 'Mitochondrial and chloroplast genomes provide insights into the evolutionary origins of quinoa (Chenopodium quinoa Willd.)', *Scientific Reports*, 9(1), pp. 1–11. Available at: https://doi.org/10.1038/s41598-018-36693-6.

Maughan, P.J. *et al.* (2024) 'North American pitseed goosefoot (Chenopodium berlandieri) is a genetic resource to improve Andean quinoa (C. quinoa)', *Scientific Reports*, 14(1), pp. 1–13. Available at: https://doi.org/10.1038/s41598-024-63106-8.

McGrath, J.M. *et al.* (2023) 'A contiguous de novo genome assembly of sugar beet EL10 (Beta vulgaris L.)', *DNA research : an international journal for rapid publication of reports on genes*

and genomes, 30(1), pp. 1–14. Available at: https://doi.org/10.1093/dnares/dsac033.

Mirarab, S., Nguyen, N. and Warnow, T. (2012) 'SEPP: SATé-enabled phylogenetic placement', in *Biocomputing 2012*. World Scientific, pp. 247–258.

Neff, E. (2017) *Developing a Molecular Pipeline To Identify Chenopodium Species in New England. Master's thesis, University of New Hampshire*. University of New Hampshire.

Neff, E., Sullivan, J.R. and Davis, T.M. (2018) 'Enhanced Documentation of Chenopodium foggii (Amaranthaceae) in Northern New England', *Rhodora*, 120(983), pp. 257–259. Available at: https://doi.org/10.3119/18-02.

Nolen, H. *et al.* (2022) 'Evaluation of Disease Severity and Molecular Relationships Between Peronospora variabilis Isolates on Chenopodium Species in New Hampshire', *Plant Disease*, 106(2), pp. 564–571. Available at: https://doi.org/10.1094/PDIS-06-21-1150-RE.

Paysan-Lafosse, T. *et al.* (2023) 'InterPro in 2022', *Nucleic Acids Research*, 51(D1), pp. D418–D427. Available at: https://doi.org/10.1093/nar/gkac993.

Rey, E. *et al.* (2023) 'A chromosome-scale assembly of the quinoa genome provides insights into the structure and dynamics of its subgenomes', *Communications Biology*, 6(1), pp. 1–14. Available at: https://doi.org/10.1038/s42003-023-05613-4.

Richard, G. (2019) 'gtrichard/deepStats: deepStats 0.3. 1 (Version 0.3. 1)', *Zenodo. doi*, 10.

Rojas, W. *et al.* (2009) 'From neglect to limelight: issues, methods and approaches in enhancing sustainable conservation and use of Andean grains in Peru and Bolivia', *Journal of Agriculture and Rural Development in the Tropics and Subtropics*, 92, p. 87.

Samuels, M.E. *et al.* (2023) 'Genomic Sequence of Canadian Chenopodium berlandieri: A North American Wild Relative of Quinoa', *Plants*, 12(3), pp. 1–23. Available at: https://doi.org/10.3390/plants12030467.

Shen, W. *et al.* (2016) 'SeqKit: A cross-platform and ultrafast toolkit for FASTA/Q file manipulation', *PLoS ONE*, 11(10), pp. 1–10. Available at: https://doi.org/10.1371/journal.pone.0163962.

Stamatakis, A. (2014) 'RAxML version 8: A tool for phylogenetic analysis and post-analysis of large phylogenies', *Bioinformatics*, 30(9), pp. 1312–1313. Available at: https://doi.org/10.1093/bioinformatics/btu033.

Stanke, M. *et al.* (2008) 'Using native and syntenically mapped cDNA alignments to improve de novo gene finding', *Bioinformatics*, 24(5), pp. 637–644. Available at: https://doi.org/10.1093/bioinformatics/btn013.

Štorchová, H. *et al.* (2015) 'The introns in FLOWERING LOCUS T-LIKE (FTL) genes are useful markers for tracking paternity in tetraploid Chenopodium quinoa Willd', *Genetic Resources and Crop Evolution*, 62(6), pp. 913–925. Available at: https://doi.org/10.1007/s10722-014-0200-8.

Štorchová, H. *et al.* (2019) 'Chenopodium ficifolium flowers under long days without upregulation of FLOWERING LOCUS T (FT) homologs', *Planta* [Preprint]. Available at:

https://doi.org/10.1007/s00425-019-03285-1.

Storer, J. *et al.* (2021) 'The Dfam community resource of transposable element families, sequence models, and genome annotations', *Mobile DNA*, 12(1), p. 2. Available at: https://doi.org/10.1186/s13100-020-00230-y.

Subedi, M. (2020) *Developing Chenopodium ficifolium as a diploid model system relevant to genetic characterization and improvement of allotetraploid C. quinoa Master's Theses and Capstones. 1407.* Available at: https://scholars.unh.edu/thesis/1407.

Subedi, M., Neff, E. and Davis, T.M. (2021) 'Developing Chenopodium ficifolium as a potential B genome diploid model system for genetic characterization and improvement of allotetraploid quinoa (Chenopodium quinoa)', *BMC Plant Biology*, 21(1), pp. 1–18. Available at: https://doi.org/10.1186/s12870-021-03270-5.

Supek, F. *et al.* (2011) 'Revigo summarizes and visualizes long lists of gene ontology terms', *PLoS ONE*, 6(7). Available at: https://doi.org/10.1371/journal.pone.0021800.

Tange, O. (2018) *GNU Parallel 2018*, *Isbn 9781387509881*. Available at: http://ole.tange.dk.

Tarailo-graovac, M. and Chen, N. (2009) 'Using RepeatMasker to Identify Repetitive Elements in Genomic Sequences', (March), pp. 1–14. Available at: https://doi.org/10.1002/0471250953.bi0410s25.

Testolin, R. and Cipriani, G. (1997) 'Paternal inheritance of chloroplast DNA and maternal inheritance of mitochondrial DNA in the genus Actinidia', *Theoretical and Applied Genetics*, 94(6–7), pp. 897–903. Available at: https://doi.org/10.1007/s001220050493.

Thorvaldsdóttir, H., Robinson, J.T. and Mesirov, J.P. (2013) 'Integrative Genomics Viewer (IGV): High-performance genomics data visualization and exploration', *Briefings in Bioinformatics*, 14(2), pp. 178–192. Available at: https://doi.org/10.1093/bib/bbs017.

Tillich, M. *et al.* (2017) 'GeSeq - Versatile and accurate annotation of organelle genomes', *Nucleic Acids Research*, 45(W1), pp. W6–W11. Available at: https://doi.org/10.1093/nar/gkx391.

Torres, A.M., Weeden, N.F. and Martín, A. (1993) 'Linkage among isozyme, RFLP and RAPD markers in Vicia faba', *Theoretical and Applied Genetics*, 85(8), pp. 937–945. Available at: https://doi.org/10.1007/BF00215032.

Vaillancourt, B. and Buell, C.R. (2019) 'High molecular weight DNA isolation method from diverse plant species for use with Oxford Nanopore sequencing', *bioRxiv*, p. 783159. Available at: https://doi.org/10.1101/783159.

Vega-Gálvez, A. *et al.* (2010) 'Nutrition facts and functional potential of quinoa (Chenopodium quinoa willd.), an ancient Andean grain: A review', *Journal of the Science of Food and Agriculture*, 90(15), pp. 2541–2547. Available at: https://doi.org/10.1002/jsfa.4158.

Vogt, F., Shirsekar, G. and Weigel, D. (2022) 'vcf2gwas: Python API for comprehensive GWAS analysis using GEMMA', *Bioinformatics*, 38(3), pp. 839–840. Available at: https://doi.org/10.1093/bioinformatics/btab710.

992 Walsh, B.M. *et al.* (2015) ‘ Chenopodium polyploidy inferences from Salt Overly Sensitive 1 (
993 SOS1) data ’, *American Journal of Botany*, 102(4), pp. 533–543. Available at:
994 https://doi.org/10.3732/ajb.1400344.

995 Wang, W., Lanfear, R. and Gaut, B. (2019) ‘Long-Reads Reveal That the Chloroplast Genome
996 Exists in Two Distinct Versions in Most Plants’, *Genome Biology and Evolution*, 11(12), pp.
997 3372–3381. Available at: https://doi.org/10.1093/gbe/evz256.

998 Wang, Y. *et al.* (2012) ‘MCScanX: A toolkit for detection and evolutionary analysis of gene
999 synteny and collinearity’, *Nucleic Acids Research*, 40(7), pp. 1–14. Available at:
1000 https://doi.org/10.1093/nar/gkr1293.

1001 Wang, Y. *et al.* (2024) ‘Detection of colinear blocks and synteny and evolutionary analyses
1002 based on utilization of MCScanX’, *Nature Protocols*, 19(7), pp. 2206–2229. Available at:
1003 https://doi.org/10.1038/s41596-024-00968-2.

1004 Ward, S.M. (1998) ‘A new source of restorable cytoplasmic male sterility in quinoa’, *Euphytica*,
1005 101(2), pp. 157–163. Available at: https://doi.org/10.1023/A:1018396808387.

1006 Warwick, S.I. and Black, L. (1980) ‘Uniparental Inheritance of Atrazine Resistance in
1007 Chenopodium album’, *Canadian Journal of Plant Science*, 60(2), pp. 751–753. Available at:
1008 https://doi.org/10.4141/cjps80-108.

1009 Wick, R.R. *et al.* (2015) ‘Bandage: Interactive visualization of de novo genome assemblies’,
1010 *Bioinformatics*, 31(20), pp. 3350–3352. Available at:
1011 https://doi.org/10.1093/bioinformatics/btv383.

1012 Young, L.A. *et al.* (2023) ‘A chromosome-scale reference of Chenopodium watsonii helps
1013 elucidate relationships within the North American A-genome Chenopodium species and with
1014 quinoa’, *Plant Genome*, 16(3): e20(April), pp. 1–17. Available at:
1015 https://doi.org/10.1002/tpg2.20349.

1016 Zou, C. *et al.* (2017) ‘A high-quality genome assembly of quinoa provides insights into the
1017 molecular basis of salt bladder-based salinity tolerance and the exceptional nutritional value’,
1018 *Cell Research*, 27(11), pp. 1327–1340. Available at: https://doi.org/10.1038/cr.2017.124.

1019

1020

1021

1022

1023

1024

1025

1026

1027

Supplemental Tables

Supplemental Table 1. Centromere positions and lengths as identified by quarTeT CentroMiner and telomere lengths and directions as identified by quarTeT TeloExplorer.

ID	Centromere			Telomere				
	Start	End	Length	Present	Upstream Length	Dir.	Downstream Length	Dir.
Cf1	58004969	58247898	242930	left	3668	+	0	
Cf2	79538569	79657117	118549	right	0		3941	-
Cf3	49844598	51718346	1873749	both	9779	+	3549	-
Cf4	39049495	40750452	1700958	both	20412	+	5019	-
Cf5	41797451	42801417	1003967	both	17843	+	3731	-
Cf6	6996291	7223985	227695	both	5397	+	4382	-
Cf7	38832653	41378639	2545987	both	882	-	5054	-
Cf8	34002546	34566367	563822	both	4480	+	5243	-
Cf9	46653552	46799075	145524	both	3710	+	4753	-

Supplemental Table 2. Positions and alleles of SNPs found in mitochondrial and chloroplast genomes used to establish maternal cytoplasmic inheritance.

Genome	Position	Reference	Alternate
Mitochondria	45844	AAAAGAATTCATTAAGAATTCACA	AA
	73300	A	C
	107870	A	C
	112616	A	C
	112987	A	C
	149592	C	T
	184591	T	A
	192086	G	T
	229731	C	A
Chloroplast	2238	T	G
Path 2	3171	C	A
	12101	C	A
	28316	CTTTTTTTTCTTTGA	CTTTTTTTCTTTGA
	30112	G	C
	30993	C	G
	33109	T	G
	42745	G	T
	49677	T	G
	50161	C	A
	63570	CAAAAAAGAAA	CAAAAAAAAAA
	64005	C	T
	67316	T	C
	81756	ATTTTTTTTTTGTT	ATTTTTTTTTGTT
	108762	G	T
	115629	A	C
	116544	A	T
	118756	C	A
	126735	C	A